Quaternary Science Reviews 106 (2014) 101–121

Contents lists available at ScienceDirect

Quaternary Science Reviews

journal homepage: www.elsevier.com/locate/quascirev

Invited review

A North Atlantic tephrostratigraphical framework for 130–60 ka b2k: new tephra discoveries, marine-based correlations, and future challenges

Siwan M. Davies [a,*], Peter M. Abbott [a], Rhian H. Meara [a,1], Nicholas J.G. Pearce [b], William E.N. Austin [c,d], Mark R. Chapman [e], Anders Svensson [f], Matthias Bigler [g], Tine L. Rasmussen [h], Sune O. Rasmussen [f], Elizabeth J. Farmer [e,2]

[a] Department of Geography, College of Science, Swansea University, Singleton Park, Swansea, Wales SA2 8PP, UK
[b] Geography and Earth Sciences, Aberystwyth University, Llandinam Building, Penglais Campus, Aberystwyth, SY23 3DB Wales, UK
[c] School of Geography and Geosciences, Irvine Building, St Andrews, KY16 9AL Scotland, UK
[d] Scottish Association for Marine Science, Scottish Marine Institute, Oban PA37, 1QA, UK
[e] School of Environmental Sciences, University of East Anglia, Norwich Research Park, Norwich NR4 7TJ, UK
[f] Centre for Ice and Climate, Niels Bohr Institute, University of Copenhagen, Juliane Maries Vej 30, Copenhagen 2100 Ø, Denmark
[g] Climate and Environmental Physics, Physics Institute and Oeschger Centre for Climate Change Research, University of Bern, Sidlerstrasse 5, 3012 Bern, Switzerland
[h] Centre for Arctic Gas Hydrate, Environment and Climate (CAGE), Department of Geology, University of Tromsø, Tromsø, Norway

ARTICLE INFO

Article history:
Received 26 November 2013
Received in revised form
24 March 2014
Accepted 27 March 2014
Available online 10 July 2014

Keywords:
Tephra
Cryptotephra
Tephrostratigraphy
Greenland ice-cores
North Atlantic marine cores
Iceland
Tephra correlations
Glass-shard analysis
Rapid climate changes

ABSTRACT

Building chronological frameworks for proxy sequences spanning 130–60 ka b2k is plagued by difficulties and uncertainties. Recent developments in the North Atlantic region, however, affirm the potential offered by tephrochronology and specifically the search for cryptotephra. Here we review the potential offered by tephrostratigraphy for sequences spanning 130–60 ka b2k. We combine newly identified cryptotephra deposits from the NGRIP ice-core and a marine core from the Iceland Basin with previously published data from the ice and marine realms to construct the first tephrostratigraphical framework for this time-interval. Forty-three tephra or cryptotephra deposits are incorporated into this framework; twenty three tephra deposits are found in the Greenland ice-cores, including nine new NGRIP tephras, and twenty separate deposits are preserved in various North Atlantic marine sequences. Major, minor and trace element results are presented for the new NGRIP horizons together with age estimates based on their position within the ice-core record. Basaltic tephras of Icelandic origin dominate the framework with only eight tephras of rhyolitic composition found. New results from marine core MD99-2253 also illustrate some of the complexities and challenges of assessing the depositional integrity of marine cryptotephra deposits. Tephra-based correlations in the marine environment provide independent tie-points for this time-interval and highlight the potential of widening the application of tephrochronology. Further investigations, however, are required, that combine robust geochemical fingerprinting and a rigorous assessment of tephra depositional processes, in order to trace coeval events between the two depositional realms.

1. Introduction

Although the Eemian interglacial serves as the most recent analogue for understanding the natural operation of the climate system during the current interglacial, the nature and pattern of the full deglaciation cycle and the subsequent return into a glaciated Earth (marine isotope stage (MIS) 6–4) are poorly understood because of the inherent difficulties of comparing palaeorecords from different depositional realms. Whilst the Eemian is thought to

* Corresponding author. Tel.: +44 1792 295233; fax: +44 1792 295324.
E-mail address: siwan.davies@swansea.ac.uk (S.M. Davies).
[1] Current address: School of Geographical and Earth Sciences, Gregory Building, University of Glasgow, Lilybank Gardens, Glasgow, G12 8QQ Scotland, UK.
[2] Current address: Department of Earth Science, University of Bergen, Allégaten 41, N-5007 Bergen, Norway.

http://dx.doi.org/10.1016/j.quascirev.2014.03.024

be a period of climatic optimum and stability (e.g. Dahl-Jensen et.al., 2013), a vast array of palaeoclimatic archives indicate that millennial/centennial-scale variability was a characteristic feature of the full MIS 6–4 period (Lototskaya and Ganssen, 1999; Oppo et al., 2001; Knudsen et al., 2002; Lehman et al., 2002; McManus et al., 2002; Shackleton et al., 2002; Heuser and Oppo, 2003; NGRIP members, 2004; Cannariato and Kennett, 2005; Capron et al., 2010; Siddall et al., 2010; Boch et al., 2011; Sanchez Goni et al., 2013; Galaasen et al., 2014). In the North Atlantic region, abrupt warmings and coolings are key features of the atmospheric changes revealed by the Greenland ice-core records (NGRIP members, 2004) (Fig. 1) and evidence from marine records uncover suborbital-scale variability during the penultimate glaciation and onset of the last glacial period (e.g. McManus et al., 1994, 1999; Chapman and Shackleton, 1999; Rasmussen et al., 1999; Knudsen et al., 2002; Shackleton et al., 2002). Yet, as a consequence of the chronological problems, an understanding of the climatic dynamics and forcing mechanisms driving these rapid events during the full spectrum of glacial/interglacial climate states, is currently unattainable.

Building chronological models for sedimentary archives, especially marine and terrestrial sequences that fall outside the radiocarbon time-frame, is limited by a scarcity of suitable radiometric dating techniques and most studies depend on a tuning approach (Lisiecki and Raymo, 2005) or simply align their records to the Greenland ice-cores and use the abrupt climatic transitions as tie-points (e.g. McManus et al., 1994; Shackleton et al., 2000; Hibbert et al., 2010; Austin and Hibbert, 2012). Although this approach allows a chronological model to be derived by assimilation of ice-core ages, the outcome precludes a comparison of independent climatic signals to test any leads and lags due to the inherent tuning assumption that abrupt climatic changes have occurred synchronously.

The same correlation challenges also affect younger sequences and in recent years tephrochronology, and the search for cryptotephra, has been recommended by the INTIMATE group[3] as a key tool to tackle these issues (Lowe et al., 2001, 2008; Blockley et al., 2012, 2014; Davies et al., 2012). A few studies have demonstrated the potential of tracing common tephras between disparate palaeoclimate archives (e.g. Grönvold et al., 1995; Davies et al., 2008; Austin et al., 2012; Lane et al., 2011) revealing how abrupt climatic changes during the Younger Dryas are time-transgressive (Lane et al., 2013) and how one millennial-scale event was synchronous between the marine and cryospheric realms during the early stages of MIS 3 (Austin et al., 2004). Very little work, however, has focused on the degree of synchronisation during older intervals characterised by different climatic boundary conditions. Tephra investigations of sequences older than 60 ka have largely focused on clearly discernible and coarse-grained marine ash zones (e.g. Sejrup et al., 1989; Sjøholm et al., 1991; Lacasse and Garbe-Schönberg, 2001; Wallrabe-Adams and Lackschewitz, 2003) and only a handful of studies has attempted to trace tephra isochrons between different cores and proxy records. (e.g. Fronval et al., 1998; Wastegård and Rasmussen, 2001; Rasmussen et al., 2003; Wastegård et al., 2005).

A shift has occurred in recent years, however, whereby investigators have sought, with great success, cryptotephra deposits in both ice-core (Abbott et al., 2012) and North Atlantic marine deposits between 130 and 60 ka b2k (Brendryen et al., 2010; Abbott et al., 2011, 2013). Tracing minute quantities of tephra material preserved within both the Greenland ice-cores and North Atlantic marine records can strengthen chronological models by incorporation of independent tephra age estimates as well as permitting the precise correlation of sequences. Not only have these studies identified several, previously unknown volcanic events, but they have also confirmed tephra correlations between marine cores. In this study nine new cryptotephra deposits, identified in the NGRIP record, and new results from MD99-2253 from the Iceland Basin, are combined with published tephra data to produce a tephrostratigraphical framework of forty-three tephra deposits for the North Atlantic region between 130 and 60 ka b2k (Fig. 1). This framework is particularly timely, allowing the well-defined cryptotephras recently outlined by Brendryen et al. (2010) and Abbott et al. (2011, 2012; 2013), to be incorporated alongside new NGRIP discoveries. What is more, a scheme of this kind is a fundamental prerequisite for establishing key time-lines between palaeoclimatic archives which then allows a test of the degree of synchronicity between atmospheric and marine proxies during the last interglacial/glacial period. We present the complete tephrostratigraphical framework first, prior to discussion of the new results, as this represents a central focal point for the paper and provides a stratigraphical and climatic context for the new tephra discoveries outlined in later sections.

2. North Atlantic tephrostratigraphical framework 130–60 ka b2k

Fig. 1 and Table 1 represent the first attempt to bring together and summarise a tephra framework for the North Atlantic region for a time-interval that has been rather overlooked in terms of its tephra potential. To do this, we follow the INTIMATE approach of Lowe et al. (2008) and Blockley et al. (2012) and present the suite of known tephras from the ice and marine records alongside the event stratigraphy outlined by Rasmussen et al. (2014). As yet, only a single tephra from this period has been identified within one of the few terrestrial deposits preserved within NW Europe (Wastegård et al., 2005) and, as such, the framework exclusively draws on tephras preserved within the available stratigraphically uncompromised Greenland ice-cores and marine realms. The framework is also constrained to the time-period preserved within the Greenland ice-cores but we note that there is significant potential to extend the marine framework further back in time.

The Greenland tephra record is based on results from Abbott et al. (2012) and new results presented in Section 2.1.2. Tephra nomenclature follows that of Davies et al. (2010), whereby the lowermost depth of the sample is used as a label e.g. the tephra at 2523.25–2523.40 m is named NGRIP 2523.40 m (see Table 2 for full depth details). If more than one geochemical population is identified within a deposit, a suffix is included after the tephra label denoting the number of sub-populations e.g. NGRIP 2944.90 m-1 and NGRIP 2944.90 m-2. Age estimates for the ice-core tephras are derived by their stratigraphic positions and the GICC05 extended timescale outlined by Wolff et al. (2010). For the latter, a modelled ss09sea age scale is employed to extend the layer-counted GICC05 chronology beyond 60 ka b2k (Svensson et al., 2008). Age uncertainties (2.5%) for each tephra are provided based on linear extrapolation of 1-sigma errors from the layer-counted part of the GICC05 timescale following the approach outlined in Abbott et al. (2012). Comparison to stalagmite records suggests that the ice-core timescale uncertainties are well within the error estimates for these independently-dated archives (Fleitmann et al., 2009; Boch et al., 2011).

For the marine realm, we draw upon several key studies and cores (Fig. 2). These include MD99-2289 from the Norwegian Sea (Brendryen et al., 2010), LINK 16, MD95-2009 and ENAM33 from the Faroes region (Wastegård and Rasmussen, 2001; Rasmussen

[3] INTIMATE: INTegrating Ice, MArine and TErrestrial records 60,000–8000 yrs b2k (EU COST Action ES0907) http://cost-es0907.geoenvi.org/.

et al., 2003; Abbott et al., 2014), MD04-2822 from the Rockall Trough (Abbott et al., 2011, 2013), and new results from MD99-2253 from the Iceland Basin (see Section 2.2.2 below). These investigations provide detailed geochemical signatures and an assessment of tephra depositional processes along with well-constrained stratigraphical placements and age estimates of the tephras relative to the Dansgaard–Oeschger cycles observed in the Greenland records (Rasmussen et al., 2014). It should be noted, however, that the relative stratigraphic position of the marine tephras shown in Fig. 1 is more informative than the age estimates that are approximations based on aligning records to the ice-cores or by tuning to a reference isotope curve (e.g. Lisiecki and Raymo, 2005) (Table 1). Tephra data reported in Sejrup et al. (1989), Sjøholm et al. (1991), Fronval et al. (1998), and Lacasse et al. (1998) are also considered and included for the construction of tephra distribution maps for the most widespread events (Fig. 2). Tephra nomenclature for the marine tephras follows that of Brendryen et al. (2010), Wastegård and Rasmussen (2001), and Abbott et al. (2013). Where coeval occurrences are found in other cores but have been given different names both names are given in Table 1.

Forty-three different tephra deposits make up the framework. Twenty of these are identified solely in the marine realm and 23 are preserved within the Greenland ice. Unsurprisingly, Iceland is the dominant source and there is an overwhelming dominance of basaltic horizons, with just 8 rhyolitic horizons identified and only one of those has been identified in the ice-cores (NGRIP 2768.45 m) (Table 1). Three horizons from Jan Mayen are also present in the framework (Brendryen et al., 2010; Abbott et al., 2012), but no tephras from more distal sources are identified. The majority of the marine tephras included in Fig. 1 and Table 1 is considered to be deposited by primary fallout or sea-ice rafting and the distribution of the most widespread tephras (5e-Eem/RHY-1 and 4-DO19s/RHY-I) is shown in Fig. 2, but, as yet, no common tephras have been traced between the ice and marine environments.

2.1. The ice-core record

2.1.1. Detection and isolation of cryptotephras

In stark contrast to mineral-rich sedimentary environments, the extraction of glass shards from cryptotephras from ice-cores is relatively straight-forward and simply involves melting the ice, centrifuging the resultant meltwater, mounting the remaining particulate material onto slides and searching for volcanic glass grains using a high-magnification light microscope (e.g. Davies et al., 2008, 2010; Abbott et al., 2012). What is challenging about this work is the necessity to process a vast number of samples to identify the cryptotephras and to carefully manipulate the small grain-sizes present for robust geochemical analysis. Initial work on ice older than 60 ka was limited to a few samples selected specifically to search for ash from the widespread Toba eruption 75 ka ago (Grönvold et al., 1995; Abbott and Davies, 2012). Since then it has become clear that the Greenland ice preserves a far more detailed and unprecedented record of volcanic events than previously identified and the laboratory-intensive work has been particularly fruitful (e.g. Mortensen et al., 2005; Davies et al., 2008, 2010; Abbott et al., 2012; Bourne et al., 2013).

Abbott et al. (2012) investigated 96.25 m of ice (985 samples) and chose to sample intervals that preserved volcanic sulphate peaks and ice that spanned abrupt warming signals (Fig. 3). Here, we adopt the same sample criteria for ice older than 70 ka and also focus on ice likely to contain known cryptotephra horizons identified in North Atlantic marine cores. This approach selected 180.4 m of ice (1089 samples) for examination (Fig. 3). Archived NGRIP ice is stored in 55-cm long pieces and a slice 2 cm^2 in cross-section was sampled along the length of each selected core-piece. This slice was further subsampled into three samples (2 × 20 cm- and 1 × 15 cm-long samples) for subsequent examination. Between 90 and 70 ka b2k each of these investigated samples represent between 12 and 17 years and increases to between 22 and 30 years beyond 105 ka b2k (Table 2). We believe that our typical 15–20 cm sampling resolution for ice-core work is sufficiently detailed to encompass most tephra or cryptotephra deposits in the ice to enable comprehensive comparison with the lower resolution records offered by the marine realm (Bourne et al., 2013). Core-pieces which contained distinct sulphate spikes were sampled at a higher-resolution to test the relationship between cryptotephra horizons and the deposition of volcanic sulphate aerosols (Davies et al., 2010; Abbott and Davies, 2012).

2.1.2. New NGRIP cryptotephras: age and geochemical signatures

The investigation of GRIP and NGRIP ice by Abbott et al. (2012) revealed the presence of deposits from 15 separate volcanic events. With just one rhyolitic tephra detected, basaltic and basaltic-andesite material dominate the deposits, which were derived from Katla, Grimsvötn, Veidivötn, Jan Mayen and unknown sources from the Icelandic rift and flank zones. These cryptotephras largely fall between 80 and 60 ka b2k and we extend this record with nine new cryptotephra deposits, details of which are provided in Fig. 1 and Table 1. The glass shards we found are brown in colour and range between 12.5 and 87.5 μm in diameter, with the smallest shard sizes found in NGRIP 2607.95 m, NGRIP 2745.60 m, and NGRIP 2944.90 m; and the largest shards were identified in NGRIP 2903.85 m (Table 2). Major and trace elements were characterised by single-grain wavelength dispersive spectrometry on the Cameca SX100 electron microprobe at the University of Edinburgh and by single-grain Laser Ablation (LA) ICP-MS (Coherent GeoLas ArF 193 nm Excimer laser ablation system coupled to a Thermo Finnegan Element 2 sector field ICP-MS) at Aberystwyth University (see Supplementary file For operating details). Electron microprobe operating conditions followed the protocol outlined in Hayward (2012) with a 15 kV accelerating voltage, 5 μm beam diameter and 2 nA beam current for Na_2O, K_2O, SiO_2, Al_2O_3, MgO, FeO (total), CaO and 80 nA beam current for P_2O_5, TiO_2 and MnO. Glass shards from both marine and ice-core records were analysed under the same microprobe operating conditions. The LA-ICP-MS analysis employed a 10 μm laser spot size and followed the methodology of Pearce et al. (2011). Two samples (NGRIP 2742.85 m and NGRIP 2745.60 m) could not be analysed by LA-ICP-MS because of a damaged sample slide and small shard sizes, respectively.

Major element results reveal that all new tephras are basaltic in composition and plot in two distinct compositional fields: transitional alkali and tholeiitic basalt (Fig. 4). The majority of shards found by Abbott et al. (2012) were also basaltic in composition. With the exception of NGRIP 2607.95 m, the major element results are tightly clustered, although outliers are evident in NGRIP 2600.60 m, NGRIP 2742.85 m, and NGRIP 2745.60 m (Fig. 4). Four shards in NGRIP 2607.95 m form a separate sub-population (referred to as NGRIP 2607.95 m-2 in Table 1 and the Supplementary information) exhibiting higher SiO_2 and total alkali values and lower MgO and CaO values than those of the main population (Fig. 4 and Supplementary information). In addition, for NGRIP 2944.90 m, eight of the analysed shards exhibit a transitional alkali composition (referred to as NGRIP 2944.90 m-1), whereas two shards plot within the tholeiitic basalt field (referred to as NGRIP 2944.90 m-2). Each sample in this interval represents around 30 years and so it is most likely that two separate volcanic events are preserved within NGRIP 2944.90 m. The single outliers for NGRIP 2600.60 m and NGRIP 2742.85 m show higher SiO_2 and plot to the right of the main tholeiitic basalt population. With just

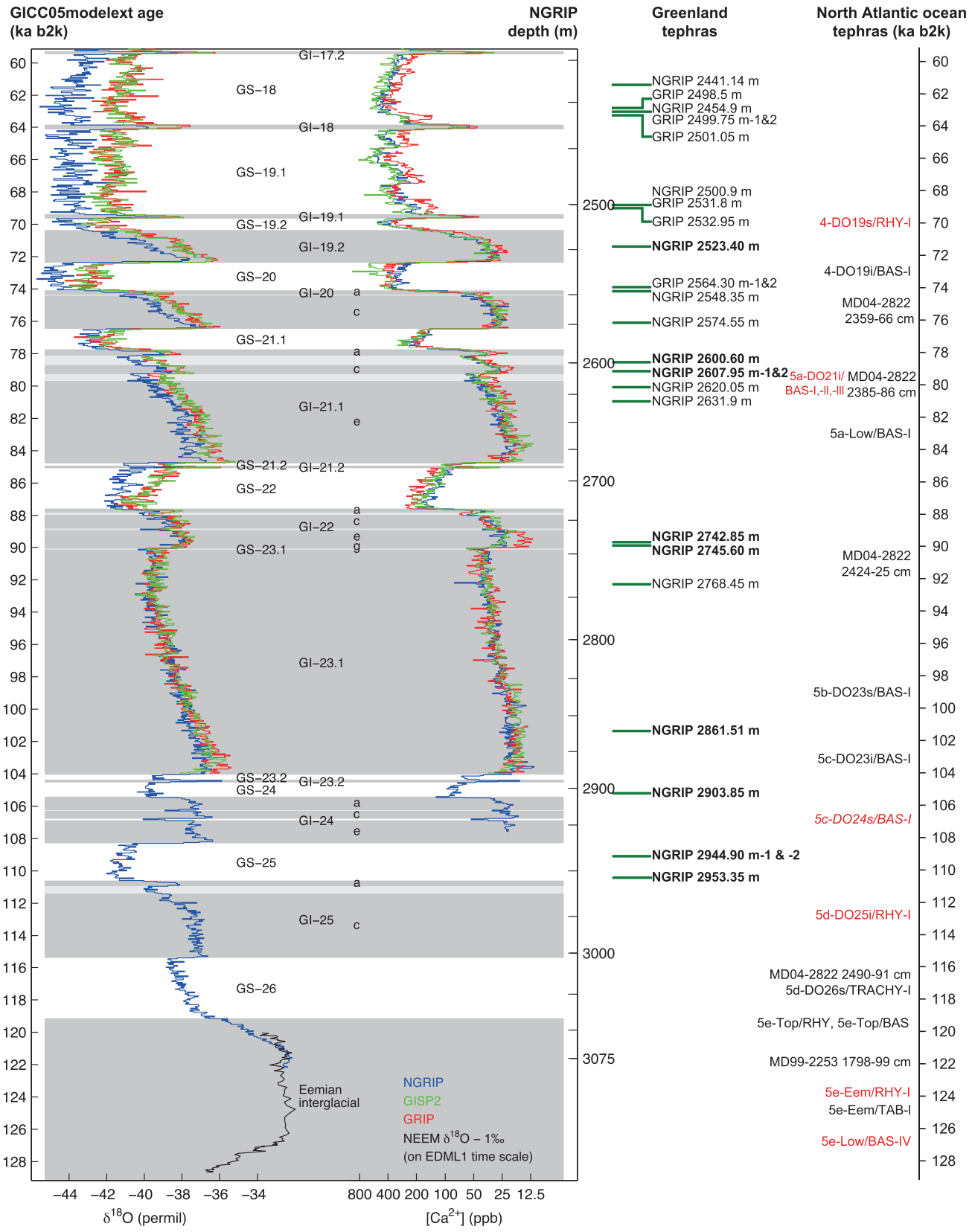

Fig. 1. Tephrostratigraphic framework for the North Atlantic region including Greenland for 130–60 ka b2k. $\delta^{18}O$ and Ca^{2+} profiles are shown against depth for NGRIP, GISP2 and GRIP and placed on the GICC05 modelext timescale (NGRIP members 2004; Wolff et al., 2010; Seierstad et al., 2014). The isotope record is extended from 122 to 129 ka based on the NEEM ice-core record shown on the EDML1 age scale (Ruth et al., 2007; Dahl-Jensen et.al., 2013). The Greenland event stratigraphy is shown alongside the oxygen isotope record with GI (interstadial) and GS (stadial) events shown according to Rasmussen et al. (2014). Cryptotephras identified in the Greenland ice-cores are from this study (**bold type**) and Abbott et al. (2012). Age estimates for the tephras are based on the GICC05 modelext timescale (Wolff et al., 2010). North Atlantic marine tephras are found within the following cores: MD99-2289 (Brendryen et al., 2010), MD04-2822 (Abbott et al., 2011, 2013), MD95-2009 and ENAM 33 (Wastegård and Rasmussen, 2001) and MD99-2253 (this study). With

Table 1
Tephra framework for the North Atlantic region 130–60 ka b2k. Marine tephras are given in italic font and tephras reported in this study are given in bold. Age estimates for the ice-core tephras are given for the base of each tephra sample and are based on the GICC05 extended timescale (Wolff et al., 2010). Age uncertainties for the ice-core ages are 2.5%. Age estimates for the marine horizons are based on publications given in the Ref. column and are largely based on comparing the climato-stratigraphic position of the tephras to the Greenland ice-core stratigraphy. The climatic event during which each tephra was deposited follows that outlined in Fig. 1. Geochemical compositions of glass shards, suggested volcanic source, and the prevailing Greenland climatic event presented in Fig. 1 are given for each tephra. Geochemical sub-populations identified are marked by suffixes e.g. −1 or −2. Bas: Basaltic; Rhy: Rhyolitic; Gr: Grimsvötn, K: Katla; JM: Jan Mayen; Ö: Öræfajökull; He: Hekla; I (SFZ/EFZ): Icelandic Southern flank zone or Eastern flank zone; V: Veidivön; Rkj: Reykjanes; V-Bá: Veidivötn-Bárdarbunga; Tr: Torfajökull; Kvl: Kverkfjöll; IRZ: Icelandic Rift Zone, EVZ: Eastern Volcanic Zone. Other names and occurrences of the tephras are provided. References are as follows: 1: this study; 2: Abbott et al. (2012); 3: Brendryen et al. (2010); 4: Abbott et al. (2011); 5: Abbott et al. (2014) 6: Wastegård and Rasmussen (2001); 7: Abbott et al. (2013); 8: Sjøholm et al. (1991); 9: Fronval et al. (1998) 10: Sejrup et al. (1989); 11 Wastegård et al. (2005).

Tephra (depth or name)	Age (yr b2k)	Climatic event	Composition	Volcanic source	Other names & occurrences	Ref
NGRIP 2441.14 m	61,410 ± 1336	GS-18	Bas andesite (tholeiitic)	IRZ		2
GRIP 2498.5 m	62,860 ± 1371	GS-18	Bas (thol)	IRZ		2
NGRIP 2454.9 m	63,090 ± 1377	GS-18	Bas/Trachybas	JM		2
GRIP 2499.75 m-1	63,090 ± 1377	GS-18	Bas/Trachybas	JM		2
GRIP 2499.75 m-2	63,090 ± 1377	GS-18	Bas (tholeiitic)	Gr		2
GRIP 2501.05 m	63,315 ± 1383	GS-18	Bas (tholeiitic)	IRZ		2
NGRIP 2500.9 m	68,900 ± 1521	GS-19.1	Bas (trans alkali)	I (SFZ/EFZ)		2
GRIP 2531.8 m	68,900 ± 1521	GS-19.1	Bas (trans alkali)	I (SFZ/EFZ)		2
GRIP 2532.95 m	69,095 ± 1526	GS-19.1	Bas (tholeiitic)	Gr-Kvl		2
4-DO19s/RHY-1	*ca 70,100*	*GS-19.2*	*Rhy (trans alkali)*	*Ö or Tr*	*MD04-2822 2327-28 cm pop 2; LINK 16 425-427 cm*	3, 4, 5
NGRIP 2523.40 m	71,445 ± 1584	GI-19.2	Bas (tholeiitic)	V		1
4-DO19i/BAS-I	*ca 72.6*	*GI-19.2*	*Bas (tholeiitic)*	*V*		3
MD04-2822 2359-66 cm	*ca73,420 ± 1770*	*GI-20*	*Rhy (tholeiitic)*	*?*		4
GRIP 2564.3 m-1&2	73,955 ± 1646	GS-20	Bas (trans alkali)	I (SFZ/EFZ)		2
NGRIP 2548.35 m	74,200 ± 1652	GI-20a	Bas (tholeiitic)	Rkj/V- Bá		2
NGRIP 2574.55 m	76,160 ± 1701	GI-20c	Bas (trans alkali)	K		2
NGRIP 2600.60 m	78,615 ± 1762	GI-21.1b	Bas (tholeiitic)	Gr		1
NGRIP 2607.95 m-1&2	79,154 ± 1775	GI-21.1c	Bas (trans alkali)	K		1
5a-DO21i/BAS I-III	*ca78,500 − 80,100*	*GI-21.1*	*Bas (tholeiitic)*	*Gr*	*5a-Top/BAS-I; LINK 16 456-57 cm*	3,5, 6
MD04-2822 2385-2386 cm	*79,600 ± 2000*	*GI-21.1*	*Rhy (trans alkali)*	*Ö*		7
NGRIP 2620.05 m	80,150 ± 1800	GI-21.1e	Bas (tholeiitic)	Gr		2
NGRIP 2631.9 m	81,030 ± 1822	GI-21.1e	Bas (trans alkali)	K		2
5a-Low/BAS-I	*ca 83,000*	*GS-22*	*Bas (tholeiitic)*	*?*		6
NGRIP 2742.85 m	89,742 ± 2038	GI-22e	Bas (tholeiitic)	Gr		1
NGRIP 2745.60 m	89,962 ± 2043	GI-22g	Bas (trans alkali)	He/K		1
MD04-2822 2424-25 cm	*91,320 ± 2410*	*GI-23.1*	*Rhy (trans alkali)*	*Ö*		7
NGRIP 2768.45 m	92,360 ± 2102	GI-23.1	Rhy (trans alkali)	I (SFZ/EFZ)		2
5b-DO23s/BAS-I	*ca 98,800*	*GI-23.1*	*Bas (tholeiitic)*	*Gr*		3
NGRIP 2861.51 m	101,448 ± 2328	GI-23.1	Bas (trans alkali)	He/Ka		1
5c-DO23i/BAS-I	*ca103,200*	*GI-23.1*	*Bas (tholeiitic)*	*Gr*		3
NGRIP 2903.85 m	105,313 ± 2424	GS-24	Bas (tholeiitic)	Gr		1
5c-DO24s/BAS-I	*ca 106,500*	*GS or GI-24*	*Bas (tholeiitic)*	*Gr*	*5c-Midt/BAS-I*	3
NGRIP 2944.90 m-1	109,217 ± 2521	GS-25	Bas (trans alkali)	He/K		1
NGRIP 2944.90 m-2	109,217 ± 2521	GS-25	Bas (tholeiitic)	Gr		1
NGRIP 2953.35 m	110,541 ± 2554	GS-25	Bas (trans alkali)	He/K		1
5d-DO25i/RHY-1	*ca 112,500*	*GI-25*	*Rhy (trans alkali)*		*5d-Low/RHY-II?*	3, 6
MD04-2822 2490-91 cm	*116,400 ± 4000*	*GI-25*	*Rhy (trans alkali)*	*Ö*		7
5d-DO26s/TRACHY-1	*ca 116,700*	*GS-26*	*Trachybasalt*	*JM*		3
5e-Top RHY; 5e-Top BAS	–	*Eemian*	*Bas & Rhy*	*EVZ*	-	6
MD99-2253 1798-99 cm	*ca 122,000*	*Eemian*	*Bas (tholeiitic)*	*?*		1
5e-Eem/RHY-1	*122,000–124,000*	*Eemian*	*Rhy*	*?*	*5e-Midt/RHY-I (see Fig 2)*	6,5,8,9,10,11
5e-Eem/TAB-1	*ca 124,400*	*Eemian*	*Bas (trans alkali)*	*K*		3
5e-Low/BAS-IV	*ca 127,000*	*Eemian*	*Bas (tholeiitic)*	*Gr*	*LINK 16 695-98 cm*	6, 5

one shard, it is difficult to determine the significance of these outliers, but their presence is recorded. The major element geochemical characterisations indicate that these cryptotephras originated from eruptions of Hekla, Katla, Grimsvötn, and Veidivötn because of their close compositional similarities (Fig. 5 and Table 1).

Rare earth element (REE) profiles exhibit a high degree of variability within each glass-shard population, particularly within NGRIP 2607.95 m, which also shows the greatest degree of scatter in the major elements (Fig. 6). Some of the variability will be analytical, associated with the small sample volumes ablated and the low elemental concentrations, whereas samples such as NGRIP 2607.95 m also show compositional variation between the glass shards analysed. Three shards analysed from population 2 of NGRIP 2607.95 m do not exhibit consistent REE profiles and these are not distinct from population 1 (Fig. 6). The greatest degree of homogeneity is shown by NGRIP 2600.60 m and NGRIP 2903.85 m with

the exception of 5c-DO24s/BAS-I, marine tephras are only included in this framework if they were likely to have been deposited by primary fallout or sea-ice rafting. 5c-DO24s/BAS-I (red italic type) is the only tephra thought to be deposited by ice-berg rafting and is found in the Norwegian Sea and Faroes region and is thus shown here for comparative purposes. Age estimates for the marine horizons are based on ages within those publications and are largely based on comparing their climato-stratigraphic position to the Greenland ice-core stratigraphy. As such the ages of the marine tephras or cryptotephras should be considered approximate. Marine tephras in red are those that have been found in more than one core. Geochemical compositions of glass and age estimates for each tephra or cryptotephra are provided in Table 1.

Table 2
NGRIP tephra depths, shard diameter and time interval (years) represented by each sample.

Tephra (depth)	Shard diameter (μm)		Time interval represented by sample (years)
	Min–Max	Mean	
NGRIP 2523.20–2523.40 m	20–60	39.5	12
NGRIP 2600.40–2600.60 m	30–45	35.67	17
NGRIP 2607.75–2607.95 m	12.5–37.5	25.83	14
NGRIP 2742.70–2742.85 m	20–57.5	41.1	12
NGRIP 2745.45–2745.60 m	17.5–42.5	26.5	12
NGRIP 2861.47–2861.51 m	32.5–55	42.25	4
NGRIP 2903.65–2903.85 m	30–87.5	52.5	22
NGRIP 2944.70–2944.90 m	15–40	25.33	30
NGRIP 2953.15–2953.35 m	15–50	28.67	29

the remaining cryptotephras exhibiting one or two outlier analyses. The latter analyses do not correspond with the outlying shards identified in the major element results.

When the average REE profiles are plotted, the cryptotephras show distinct patterns reflecting different sources and these support the assignations established by major elements (Fig. 7). NGRIP 2523.40 m, NGRIP 2600.60 m, and NGRIP 2903.85 m display a rather flat REE gradient and fall within the compositional envelope for bulk samples from Veidivötn-Bárdarbunga and Grimsvötn defined by Meyer et al. (1985) and Óladottir et al., 2011 (Fig. 7). These cryptotephras also plot within La–Lu and La–Yb envelopes or on the same trend of glasses analysed from these source volcanoes (Fig. 7). In contrast to the Veidivötn-Bárdarbunga and Grimsvötn tephras, material from NGRIP 2607.95 m-1, NGRIP 2861.51 m, NGRIP 2944.90 m-1, and NGRIP 2953.35 m show a slightly steeper REE profile akin to the proximal characterisations of bulk glass samples erupted from Hekla and Katla presented by Meyer et al. (1985) (Fig. 7). The overall concentrations, however, are lower in the distal ice-core samples relative to the proximal material from Iceland. This difference is also observed in the La–Lu and La–Yb biplots, but the analyses seem to fall on the same trend determined by Meyer et al. (1985). The offset in numerical values for the Hekla-Katla tephras may well reflect methodological differences between the analysis of bulk material by instrumental neutron activation analysis (which may be affected by the presence of microlite inclusions) and single-grain analysis of glass by LA-ICP-MS. Alternatively, the proximal deposits may represent more evolved material. Although the Meyer et al. (1985) envelopes are much narrower, the NGRIP tephras thought to be sourced from Hekla and Katla plot within the same area on ratio–ratio plots and can be clearly discriminated from the Veidivötn and Grimsvötn tephras (Fig. 7). To date, comparisons of distal and proximal trace element compositions are limited by a scarcity of LA-ICP-MS proximal data-sets. Nonetheless, the trace element results strengthen the source correlations suggested by major element results and the full geochemical characterisations presented for glass shards from these tephras provides an invaluable fingerprint for future comparisons.

Thus, in total 23 tephra deposits make up the Greenland tephra record during this time-interval (Fig. 1). Although the tephras are not shown in Fig. 1, Grönvold et al. (1995) also reported the preservation of three closely-spaced deposits around 80 ka b2k in GRIP and one of these may correlate to the visible NGRIP 2631.9 m horizon outlined by Abbott et al. (2012), although limited geochemical results prevents a rigorous comparison. Nineteen tephras in this framework are found in the 60–95 ka interval with only four tephras found between 95 and 130 ka. Although ice for NGRIP only extends back to 123 ka b2k, there is a stark contrast between the ashfall frequency in the early and later stages of this interval, which may reflect a more intense sampling effort in the younger part of the record rather than a difference in volcanic activity or dispersal (Fig. 3).

A number of these tephras were deposited close to times of rapid climatic changes. For instance, NGRIP 2548.35 m, NGRIP 2903.85 m, and NGRIP 2953.35 m were deposited close to the sharp cooling transitions of GI-20a, GI-24a and GI-25a, respectively, and NGRIP 2574.55 m and NGRIP 2745.60 m and 2742.85 m were deposited close to the abrupt warming that marks the start of a Greenland Interstadial (Fig. 1). Furthermore, NGRIP 2607.95 m and NGRIP 2600.60 m fell either side of the short-lived climatic oscillation GI-21.1c. Further discussion of the potential of these individual tephras as chronostratigraphic markers is provided below in Section 3.

2.1.3. Tephras and ice chemo-stratigraphy

Sulphate concentrations and changes in the acidity of the ice from the fallout of sulphuric acid have long been used as proxies for volcanic events in the ice-core records (Zielinski et al., 1996, 1997; Severi et al., 2007; Gao et al., 2008; Parrenin et al., 2012), yet recent studies reveal that glass shards derived from a tephra-generating eruption can be present in the ice without a coeval sulphate spike (Davies et al., 2010; Abbott and Davies, 2012; Abbott et al., 2012; Coulter et al., 2012). Some have suggested that these occurrences may be due to the neutralisation of acid fallout by the volcanic glass (Palais and Kyle, 1988), whereas others have explained small stratigraphic offsets between aerosol and glass-shard deposition via differential transport pathways (Fiacco et al., 1993, 1994). The sampling resolution adopted in this study is too coarse to allow an investigation of such short-lived offsets. Instead we compare the expression of chemical signals in NGRIP ice (sulphate, electrolytical meltwater conductivity, calcium and dust derived from continuous flow analysis: Bigler (2004)) in relation to the position of seven cryptotephras. Chemical stratigraphic data were not obtained deeper than 2930.4 m and so are unavailable for comparison to the positions of NGRIP 2944.90 m and 2953.35 m. A comparison of tephra positions relative to this suite of chemical indicators allows an insight into the complexities associated with sulphate concentrations in ice-core records and the competing influences of dust inputs, sea salt, biogenic sources and dimethyl sulphide as well as inputs from volcanic eruptions (Fig. 8).

In general, the prevailing climatic conditions are thought to be crucial in determining whether tephra deposition onto ice coincides with a response in the ice chemistry. Ice during warm episodes tends to be more acidic due to the reduced input of alkaline dust. What is more, background levels are low and natural variability is low during warm episodes whereas background sulphate levels and natural variability are higher during cold episodes (e.g. see Fig. 3 of Svensson et al., 2013). Consequently, volcanic sulphate spikes during warm episodes are thought to be more pronounced and detectable whereas during cold events, any volcanic sulphate is swamped and the sulphate concentrations are more likely to reflect deposition from dust episodes rather than from volcanic aerosols that may indicate the deposition of tephra particles (Steffensen, 1995; Svensson et al., 2013). Although our interpretations are somewhat limited by data availability, this simple relationship is not so clear in the results outlined in Fig. 8 and those presented in other studies (e.g. Davies et al., 2010; Abbott et al., 2012).

Four of the tephras with complete CFA data-sets fell during warm episodes. During the warm GI-23.1 event, clear sulphate (~250 ppbw), calcium, and conductivity peaks are observed in association with the NGRIP 2861.51 m tephra-derived glass occurrence (Fig. 8). This particular core-piece was sampled at a higher resolution due to the presence of this sulphate peak and the tephra itself is constrained to a 4-cm sample which is equivalent to four

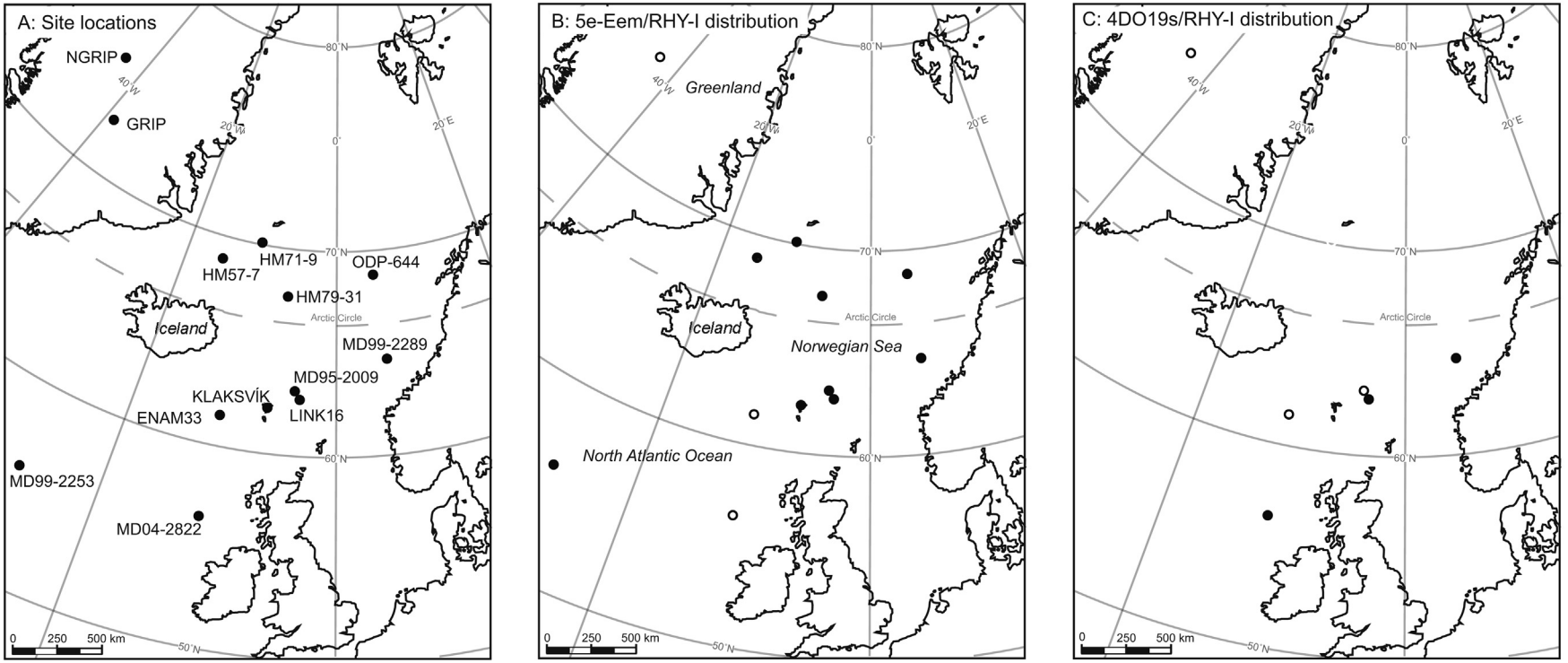

Fig. 2. A) Location of core sites mentioned in the text. B & C) Distribution of the most widespread tephras, 5e-Eem/RHY-I and 4-DO19s/RHY-I, respectively. Closed circles denote the core locations where these tephras have been identified, whereas open circles represent sites that have been investigated according to the likely age of a particular tephra but where no tephra has been identified. For references associated with these tephra findings see Table 1 caption.

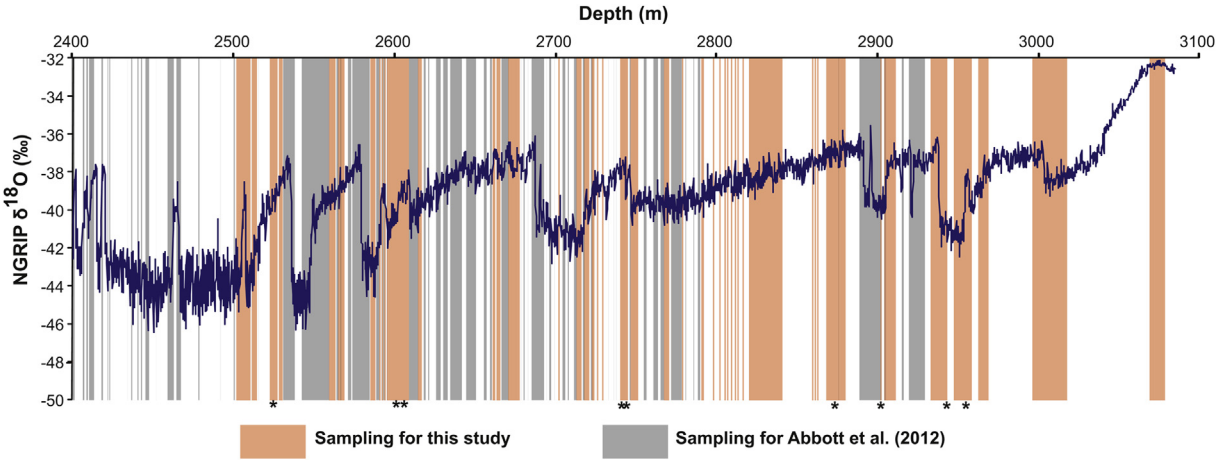

Fig. 3. Sampling strategy for the NGRIP ice-core for this study and for Abbott et al. (2012) plotted against the oxygen isotope record (NGRIP members, 2004). Core intervals left white have not been sampled for glass analysis. * = tephra positions identified in this study.

years of ice/snow accumulation (Table 2). Mineral dust input at this time is reduced relative to that associated with cold stadial episodes (see for example the dust input for NGRIP 2903.85 m and 2600.6 m). This reduction is consistent with the expected change in ice-core chemistry following a volcanic eruption during warm climatic conditions. Smaller sulphate, calcium, and conductivity peaks coincide with NGRIP 2607.95 m, NGRIP 2745.6 m, and NGRIP 2742.85 m which were also deposited during warm episodes. Although we have not pinpointed the exact positions of the tephra within these 15- and 20- cm –long ice-core samples, the peaks seen in these samples are likely to relate to these volcanic events. It should be noted, however, that the small peak in sulphate and conductivity between 2742.7 and 2742.85 m is no more significant than background levels.

Abbott et al. (2012) also observed modest sulphate peaks of ~120–300 ppbw in association with tephras deposited during warm episodes, with others revealing no coeval sulphate signal at all. In stark contrast, NGRIP 2454.9 m and NGRIP 2500.9 m were deposited during cold episodes, and the glass-shard concentrations coincide with high sulphate peaks in excess of 2000 ppbw and 600 ppbw, respectively (Abbott et al., 2012). Davies et al. (2010) also highlighted a similar inconsistent relationship between tephras deposited during cold and warm episodes. For comparative purposes, only one tephra with a complete CFA data-set was deposited during a cold episode in the suite of samples presented here (NGRIP 2903.85 m). For this sample, no response is observed in the chemical indicators, but the position of the glass falls, by a few centimetres, after a sulphate peak of ~250 ppbw. This offset may well be an artefact of small depth offsets between the CFA samples versus actual core depths resulting from the procedures adopted for CFA core-processing. Thus, our interpretations are somewhat limited with only one cold-episode example presented here, but the chemical expression of tephra deposition presented elsewhere does not seem to follow a simple climatic-driven relationship (Davies et al., 2010; Abbott et al., 2012). The relationship between tephra deposition and coeval volcanic aerosol fallout is clearly complex and, contrary to the findings of previous studies, is not solely controlled by prevailing climatic conditions. For instance, the spatial variability of snow deposition and volcanic ash fallout may also significantly influence the height and shape of volcanic aerosol signals in the ice (Wolff et al., 2005; Coulter et al., 2012). What is shown by the data, however, is that high-magnitude aerosol peaks are not always indicators of nearby Icelandic eruptions and the chemical indicators from the latter are sometimes no more significant than background levels in an ice-core record. Thus sampling strategies for cryptotephra investigations cannot rely solely on targeted searches guided by large chemical spikes and likewise volcanic frequency studies may underestimate the past eruptive frequency based exclusively on the most significant chemical imprints preserved in the ice.

2.2. The marine record

2.2.1. Detection of marine cryptotephra deposits and potential links to the ice

Identification of cryptotephra deposits in the marine environment requires a systematic and contiguous down-core investigation. Shorter core lengths, relative to the ice-cores, allow full sequences to be investigated for cryptotephra deposits. Two different approaches have been adopted to identify the marine cryptotephra deposits outlined in Fig. 1. Firstly, Fronval et al. (1998), Wastegård and Rasmussen (2001), and Brendryen et al. (2010) investigated the tephra content by simply sieving the sediment into different size fractions and counting the number of glass shards within the respective size fraction. Wastegård and Rasmussen (2001) reported all shards >150 μm in size whereas Brendryen et al. (2010) counted the number of shards present within the 63–125 μm (also the component investigated by Fronval et al. (1998)) and 125–150 μm grain-size fractions. This approach has identified several tephras such as the widespread 5e-Eem/RHY-I, 5d-DO25i/RHY-I, 5a-DO21i/BAS-I–III and the 4-DO19i/BAS-I (Fig. 1). Further examination of finer-grained components allows the isolation of cryptotephra deposits (glass shard concentrations) that may be present. This alternative approach incorporates wet sieving at different grain-size fractions (25 μm, 80 μm, and 125 μm) with a density separation technique to isolate any rhyolitic material that may be present in the 25–80 μm fraction (Turney, 1998). This is a technique widely used on mineral-rich lacustrine sediments but its use in a North Atlantic marine context has, to date, only been employed by Abbott et al. (2011, 2013, 2014). These latter studies have successfully identified several, previously unknown deposits such as the series of rhyolitic horizons in MD04-2822 (Abbott et al., 2011, 2013) (Fig. 1). The denser fraction (>2.5 g/cm^3) remaining after density separation can also be examined for basaltic shards (Abbott et al., 2014) and magnetic separation is also being increasingly utilised to purify this fraction (Griggs et al., 2014). Although not applied to tephras in the time-interval under consideration here, some studies have also demonstrated how magnetic measurements on bulk sediment can identify cryptotephra deposits within marine sediments (Peters et al., 2010).

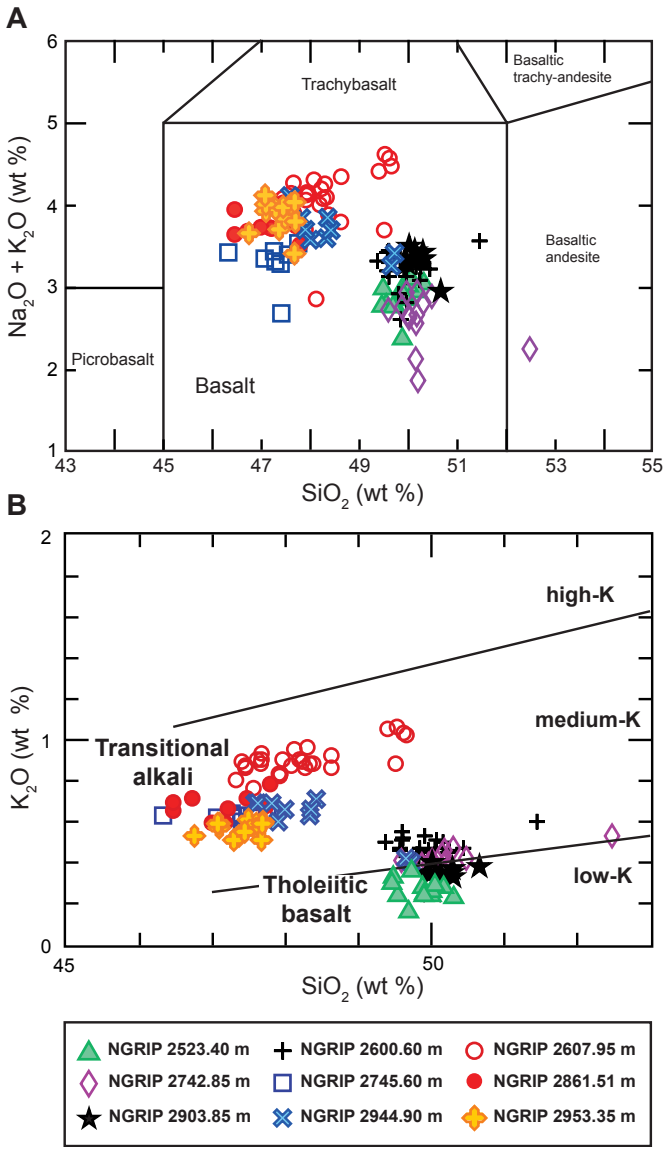

Fig. 4. Geochemical classification for analyses of glass shards from the NGRIP tephras identified in this study. A: Total alkali versus SiO_2 plot following the chemical classification outlined by Le Maitre (1989). B: SiO_2 versus K_2O biplot highlighting the tholeiitic and transitional alkali populations. Data shown are normalised values. Full data-set available in the Supplementary information.

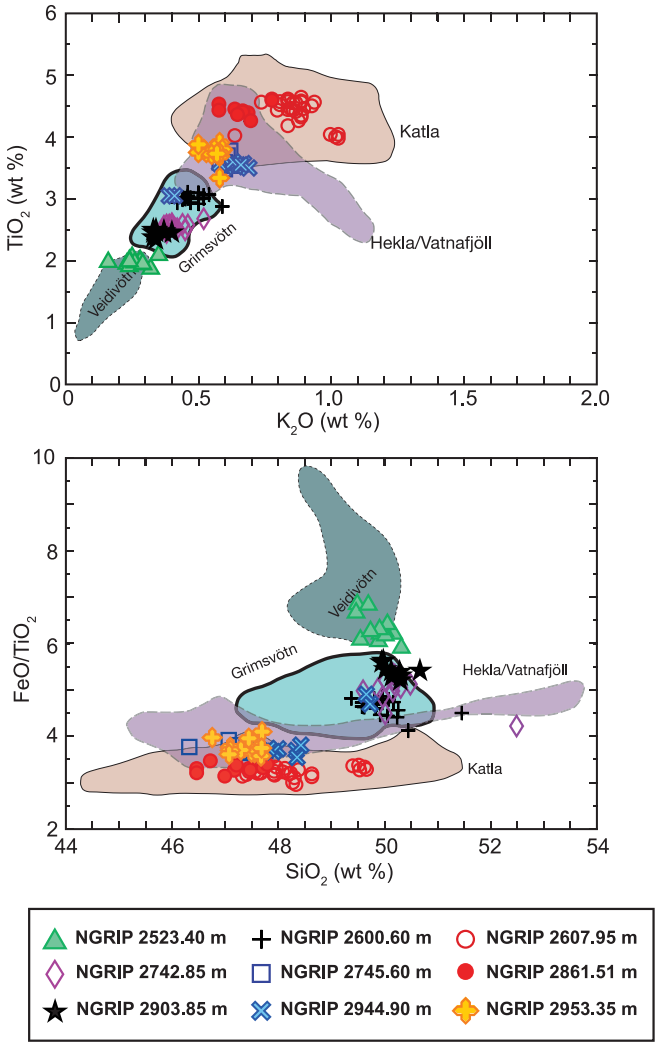

Fig. 5. Major element results for glass shards analysed from the NGRIP cryptotephras identified in this study versus the main Icelandic source volcano envelopes for glasses. Volcanic envelopes are based on geochemical results presented in Jakobsson (1979), Boygle (1994), Hunt et al. (1995), Dugmore and Newton (1998), Haflidason et al. (2000) and references within, Davies et al. (2001), Wastegård et al. (2001), Larsen et al. (2002), Andrews et al. (2002), Mortensen et al. (2005), Óladóttir et al., 2008. Data shown are normalised values and total Fe is reported as FeO.

The application of these different methods has led to the identification of 20 separate deposits in the marine environment including new discoveries outlined here in MD99-2253 (Section 2.2.2). Some of the marine tephras have been matched between a number of cores (Figs. 1 and 2). For instance, the 5e-Eem/RHY-I (also referred to as 5e-Midt/RHY) has been identified in cores from north of Iceland (Sejrup et al., 1989; Sjøholm et al., 1991; Fronval et al., 1998), the Faroe Islands region (both marine and terrestrial sequences) (Wastegård and Rasmussen, 2001; Wastegård et al., 2005), and the Norwegian Sea (Brendryen et al., 2010) (Fig. 2). A more recent discovery extends the distribution of the 4-DO19s/RHY-I tephra from the Norwegian Sea into the Faroes region and the Rockall Trough (Brendryen et al., 2010; Abbott et al., 2014). Other tephras including the 5d-DO25i/RHY-I, the 5a-DO21i/BAS I-III, and 5c-DO24s/BAS-I have been identified in at least two cores in the Norwegian Sea and Faroes region (Brendryen et al., 2010; Abbott et al., 2014). The last (5c-DO24s/BAS-I) is thought to be an iceberg-rafted deposit, and is only included within this framework, as a crude event marker between marine cores.

Several tephras in Fig. 1 are based on occurrences in single cores such as four horizons in MD04-2822 (Abbott et al., 2013) and 1798-99 cm within MD99-2253 (see below). These recent findings emphasise the value of investigating marine cores for the presence of cryptotephras and highlight that this type of work is very much in its infancy. Fig. 2 emphasises how few core sections spanning this interval have actually been examined for the presence of tephras and cryptotephra deposits. Moreover, our work on MD99-2253 demonstrates the potential of extending the distribution of some key tephras further west into the North Atlantic and also that such records may preserve an untapped record of volcanic events.

Widening the search to other cores from different regions of the North Atlantic will enable the distribution of different tephra-fall deposits to be better ascertained. What is more, further marine work may well lead to the identification of some of the ice-core tephras outlined here. As yet, the only suggested tephra of similar geochemical signatures and stratigraphical position that could be

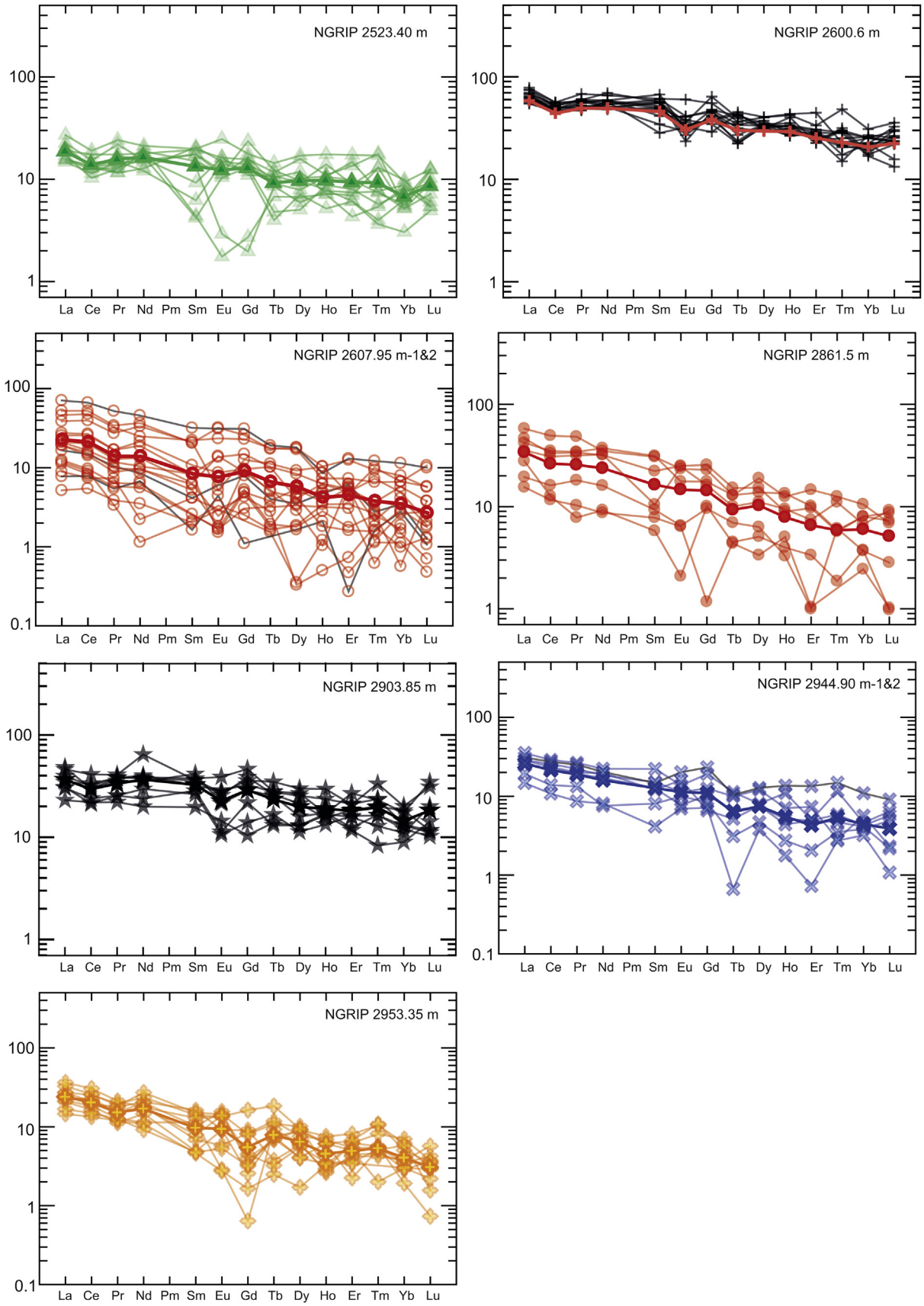

Fig. 6. Chondrite-normalised REE profiles for glass shards from seven NGRIP tephras analysed by LA-ICP-MS. Chondrite composition from Sun and McDonough (1989). Profiles for individual shards as well as the average REE profile (bold type and red for NGRIP 2600.6 m) are presented for each deposit. REE profiles for glass shards from the sub-populations NGRIP 2607.95 m-2 and NGRIP 2944.90 m-2 are shown by grey lines. Any outlier shards and sub-populations observed in the major elements are not included in the trace elemental averages. Full data-set available in the Supplementary information.

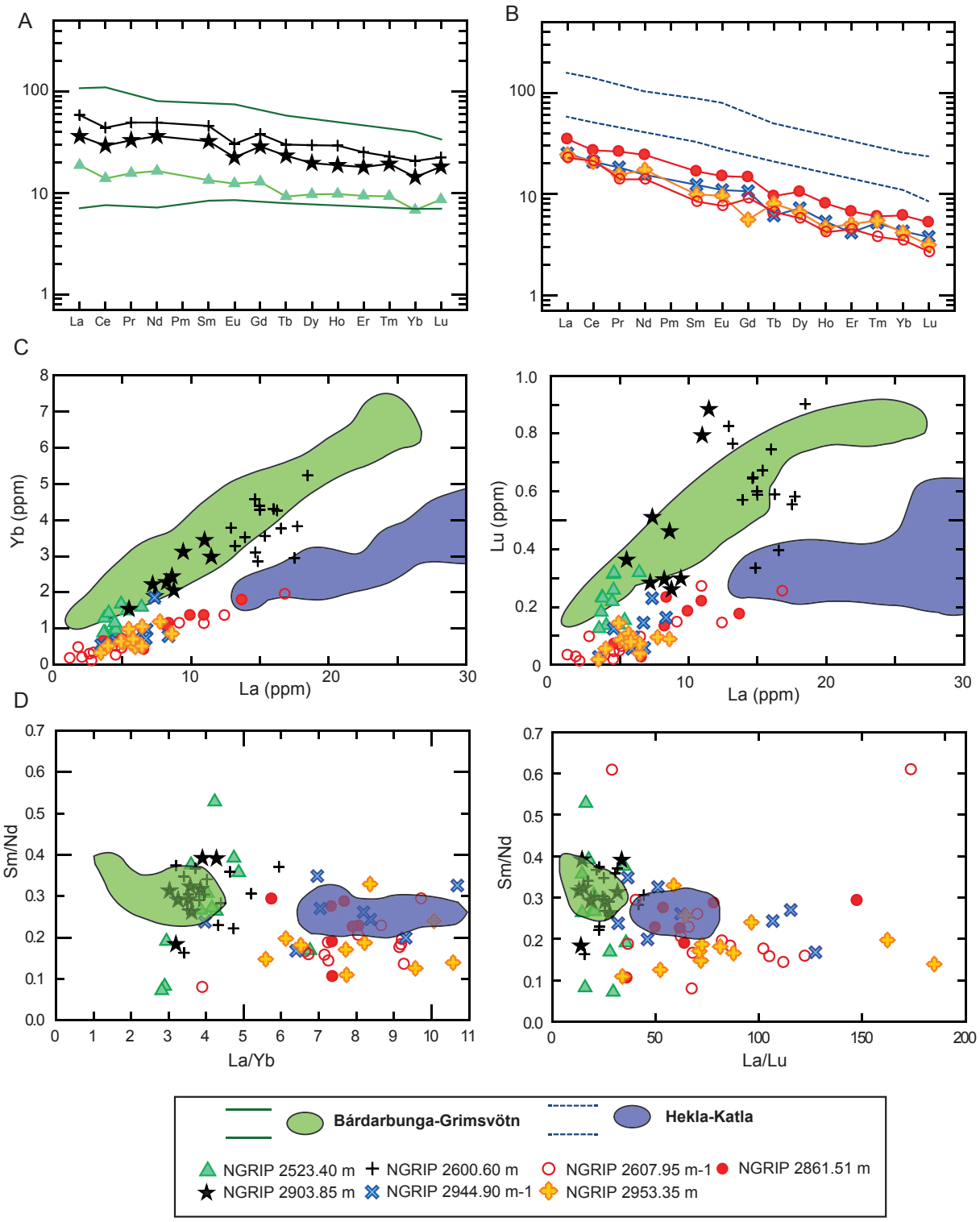

Fig. 7. Trace element characterisations and source assignation of glass shards from seven NGRIP tephras analysed by LA-ICP-MS. Trace elemental averages shown do not include any outliers or sub-populations. A: Average chondrite-normalised REE profile for Veidivötn and Grimsvötn tephras identified in NGRIP (bold type profiles in Fig. 6). B: Average chondrite normalised REE profile for Hekla & Katla tephras identified in NGRIP (bold type profiles in Fig. 6). Chondrite composition from Sun and McDonough (1989). C: Biplots of La vs Yb and La vs Lu for the seven NGRIP tephras analysed by LA-ICP-MS. Numerical concentrations are presented. D: Trace element ratio–ratio plots for La/Yb versus Sm/Nd and La/Lu versus Sm/Nd. Source envelopes are from Meyer et al. (1985) and Óladottir et al. (2011).

traced between the two realms is that of NGRIP 2631.9 m and EW9302-12JPC (527-29 cm) (Lacasse et al., 1998; Abbott et al., 2012). Limited stratigraphical information and proxy evidence from the marine environment, however, prevents a firm correlation. Beyond 80 ka b2k, several tephras with a Grimsvötn-type glass chemistry are found in both NGRIP and MD99-2289 (Brendryen et al., 2010). Geochemical comparisons of glass from these tephras are shown in Fig. 9 which highlights no consistent

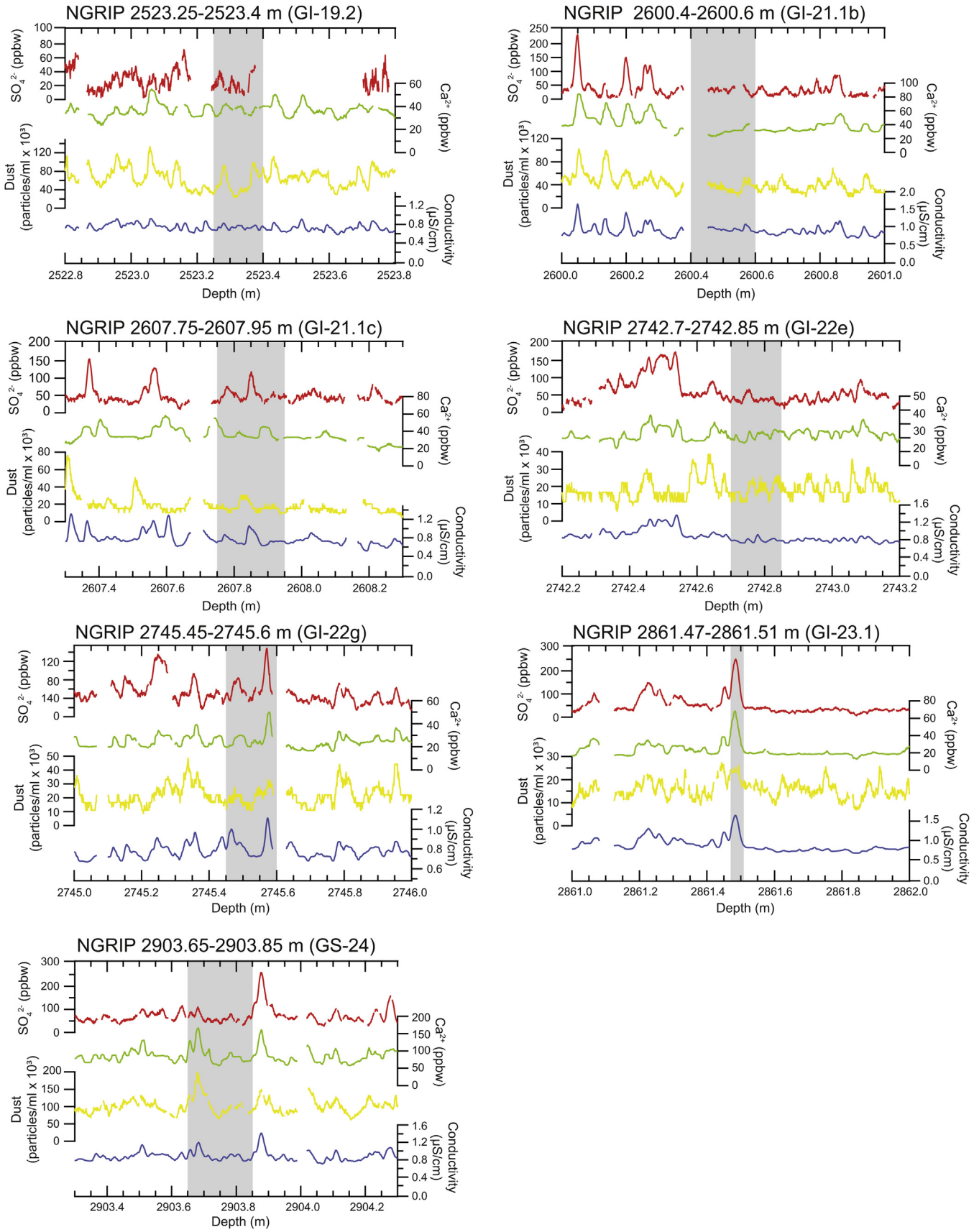

Fig. 8. NGRIP ice-core chemostratigraphy in association with cryptotephra positions. Sulphate, calcium, electrolytic meltwater conductivity, and dust analyses have been measured by the continuous flow analysis (CFA) system. Tephra positions are shown by the grey shaded areas. No CFA data are available below 2930.4 m thus preventing a comparison to the tephras at 2944.90 m and 2953.35 m. The associated Greenland Interstadial (GI) or stadial (GS) episode is marked for each tephra.

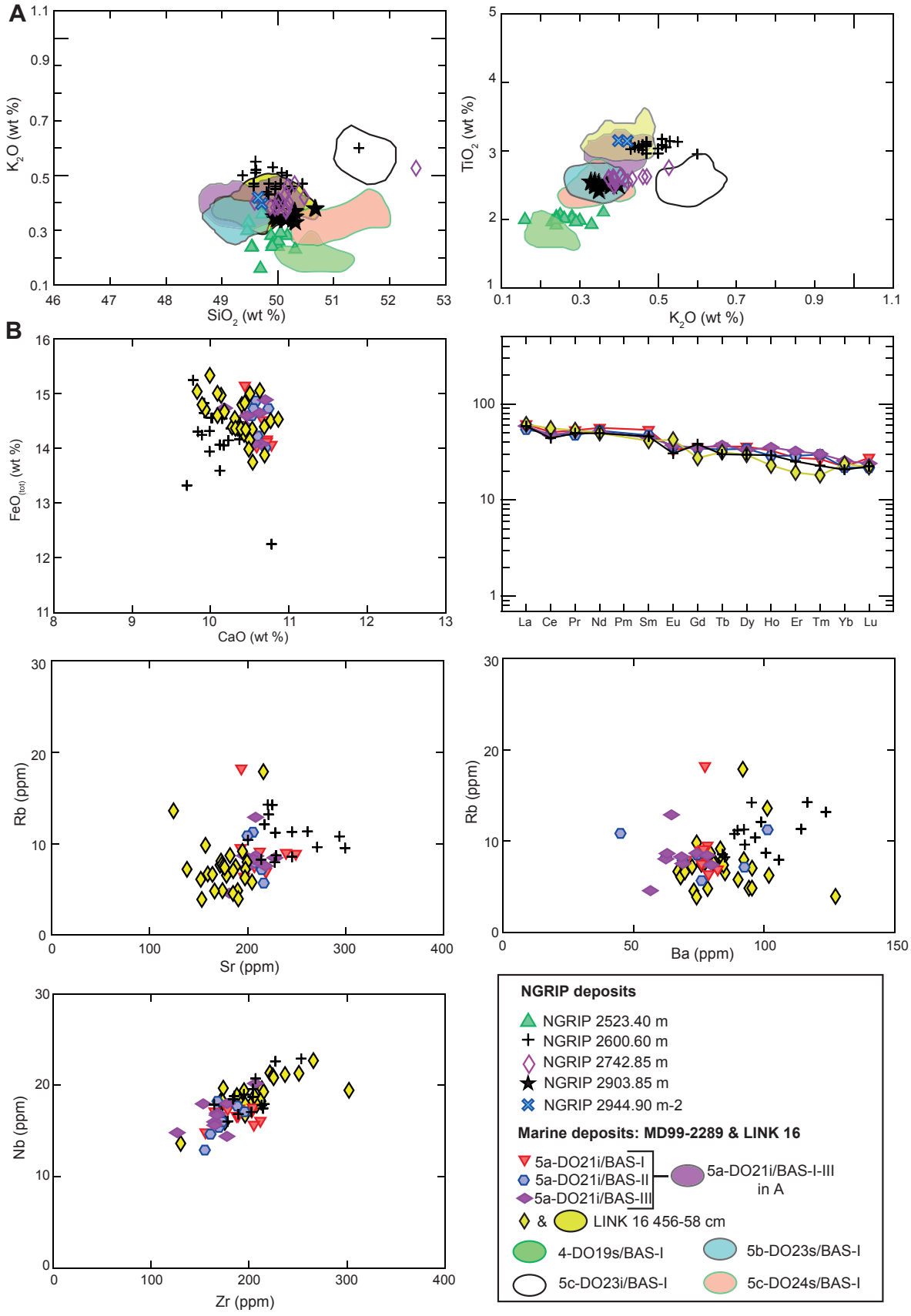

Fig. 9. Geochemical comparisons of analyses from five NGRIP tephras of basaltic tholeiitic composition with those of marine tephras of Veidivötn and Grimsvötn origin from Brendryen et al. (2010) and Abbott et al. (2014). The marine tephras are as follows: 4-DO19s/BAS-I, 5a-DO21i/BAS-I, 5a-DO21i/BAS-II and 5aDO21i/BAS-III, 5b-DO23s/BAS-I, 5c-DO23i/BAS-I, and 5c-DO24s/BAS-I. For clarity on the biplots, glass analyses for 5a-DO21i/BAS-I,/BAS-II and/BAS-III are combined to show one overall envelope as the individual deposits are indistinguishable on major elements. A: SiO_2 vs K_2O (wt%) & K_2O vs TiO_2 (wt%). B: CaO vs FeO_{tot} (wt %) biplot, chondrite-normalised REE profile and Sr vs Rb, Ba vs Rb and Zr vs Nb biplots for NGRIP 2600.6 m and 5aDO21i/BAS-I, 5aDO21i/BAS-II, 5a-DO21i/BAS-III (re-analysed in Abbott et al. 2014), and LINK 16 456-58 cm (Abbott et al. 2014). Chondrite compositions from Sun and McDonough (1989). Major elements are normalised and total Fe is reported as FeO.

geochemical relationship between NGRIP 2742.85 m, NGRIP 2903.85 m and NGRIP 2944.90 m-2 and 5c-DO24s/BAS-I, 5c-DO23i/BAS-I and 5b-DO23s/BAS-I. In addition, 4-DO19i/BAS-I and NGRIP 2523.40 m share a common volcanic origin and are close in age, but there is no consistent overlap in geochemical analyses of associated glass with offsets seen in SiO_2, MgO, and Al_2O_3 concentrations (Fig. 9 & Supplementary information).

Similar glass-based geochemical signatures and a common stratigraphic position also suggest a possible correlation between NGRIP 2600.60 m tephra and the 5a-DO21i/BAS I-III tephras (Figs. 1 and 9). The latter group was described as a tephra zone in sediments in the Norwegian Sea with three distinct and closely-spaced peaks in glass-shard concentration (Brendryen et al., 2010). Glasses from the three peaks are indistinguishable according to the major element and trace element signatures obtained from them (Brendryen et al., 2010; Abbott et al., 2014), and the entire deposit consequently is thought to correlate to the 5a-Top/BAS-I described by Wastegård and Rasmussen (2001). Abbott et al. (2014) describe a deposit at 456–458 cm within the LINK 16 marine core (Fig. 2) which they also believe is related to the 5a-DO21i/BAS I-III deposit but represents fallout from a different eruptive phase. This is revealed by differences in the major and trace element data which are consistent with a fractional crystallisation link between the LINK 16 and MD99-2289 deposits (Abbott et al., 2014). Here, some glass shards from the NGRIP 2600.60 m deposit show good correspondence with the overall 5a-DO21i/BAS I-III envelope and the LINK 16 456–458 cm deposit (Fig. 9). However, other shards from this NGRIP population have higher K_2O values and lower CaO concentrations and the trace elements show higher Rb, Ba and Sr values (Fig. 9). Thus, despite the similar REE profile and incompatible trace element ratios (e.g. Zr/Nb, Hf/Ta and Zr/Th), we do not believe that the NGRIP 2600.60 m tephra correlates to the 5a-DO21i/BAS I-III tephras and the former is unlikely to represent a different eruptive phase. Higher K_2O and lower CaO concentrations in NGRIP 2600.60 m are inconsistent with higher Sr contents, which cannot be generated by a realistic fractional crystallisation model (plagioclase ± clinopyroxene ± olivine) to link the ice and marine tephra occurrences. For instance, plagioclase extraction would remove both Ca and Sr from the melt (i.e. lower concentrations in the tephra, not exhibited by Sr) and result in higher K_2O, Ba and Rb values. Instead we believe that they most likely originate from the same source but represent separate eruptions. This is a key example of how subtle geochemical variations should be scrutinised in both major and trace elements to ascertain a robust correlation. What is more, it is clear that Grimsvötn was a major producer of tephra during the last glacial period and thus emphasises the imperative need for careful acquisition of geochemical data. Some key recommendations include data acquisition under the same operating conditions (if possible the same microprobe) with regular analyses of appropriate reference materials (Bourne et al., 2013; Pearce et al., 2014; Abbott et al., in 2014). Cryptotephra work conducted in distal regions has revealed a far more detailed record of eruptions than previously recognised, and thus, re-affirms the necessity to scrutinise and carefully examine tephra geochemical signatures.

2.2.2. *Assessing the integrity of cryptotephras in the marine environment and new results from MD99-2253*

With further work expected in this area, the major challenge for marine work is assessing the stratigraphic integrity of the horizons identified and hence their reliability as isochronous marker beds or tie-points. This is especially relevant for cryptotephras that are composed of a low concentration of glass shards resulting in their invisibility within the host material. Cryptotephra deposits are not characterised by a sharp basal contact akin to that observed with visible layers (cf. Lacasse et al., 1998), but instead typically reveal a distinct increase in shard concentration followed by a declining tail and a gradational upper boundary which can only be detected by isolation techniques performed in the laboratory. Thus, determining the peak glass concentration is an essential first step for any cryptotephra work in the marine and other sedimentary realms. Indeed, cryptotephra deposits in the marine environment are particularly vulnerable to the 'competing' influences of other depositional processes such as iceberg rafting, bioturbation, and ocean current redistribution. As a result, a combination of key diagnostic features (e.g. shard concentration profiles, grain-size distribution, geochemical homogeneity, and co-variance with ice-rafted detritus (IRD) input) require thorough investigation in order to assess the depositional history of a cryptotephra deposit and thus, its value as an isochronous marker horizon or chronostratigraphic tie-point (see e.g. Brendryen et al., 2010; Kuhs et al., 2014; Griggs et al., 2014).

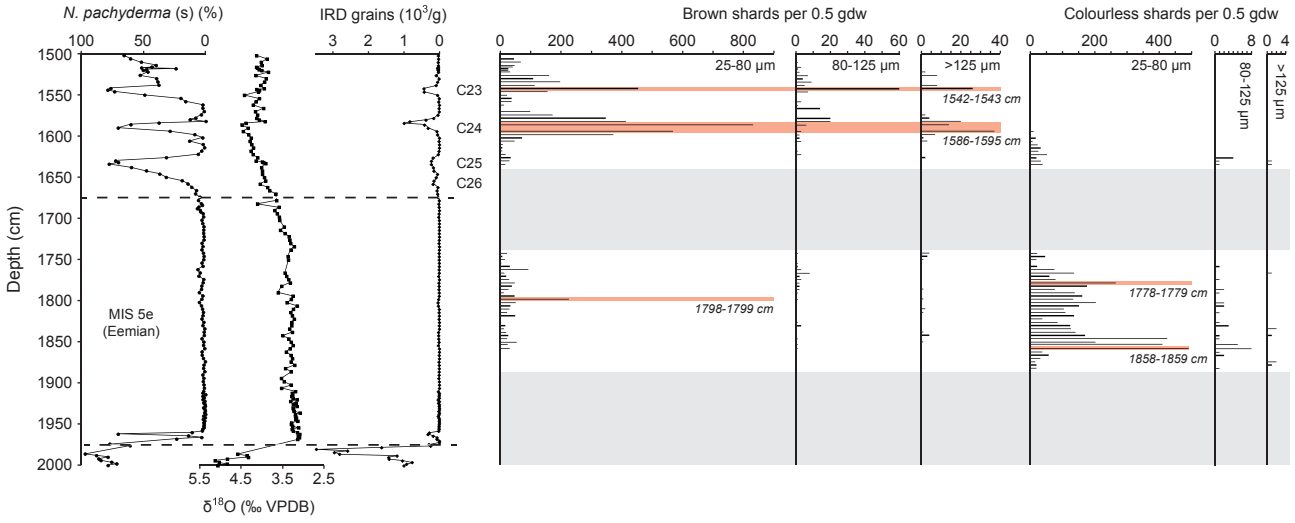

Fig. 10. Glass shard concentrations for MD99-2253. Colourless and brown shards identified microscopically are presented for each grain-size fraction. *Neogloboquadrina pachyderma* (s) percentage abundances, benthic oxygen isotope data, and concentration of IRD grains are also shown. Red bars denote depth intervals from which glass shards were extracted for geochemical analysis. Cooling events (C26–C24) associated with ice rafting episodes follow the nomenclature of Chapman and Shackleton (1999).

New results are presented from core MD99-2253 on the Gardar Drift (56°21.78′N, 27°48.95′W; water depth 2840 m) (Fig. 2) to demonstrate how some of these diagnostic features are employed to isolate and assess the stratigraphic integrity of cryptotephra deposits in these cores (Fig. 10). Sediment samples at 2-cm intervals were investigated between 15 and 16.4 m and between 17.5 and 18.75 m, specifically selected according to sample availability and the stratigraphic juxtapositions of tephras identified elsewhere in the NE Atlantic during the Eemian and the glacial transition (e.g. Rasmussen et al., 2003; Brendryen et al., 2010). Wet sieving of different grain-size fractions and subsequent density separation of the 25–80 μm material revealed distinct peaks of high glass concentrations in this fraction (Fig. 10). In the lowermost interval, colourless rhyolitic shards peak at 1858–1859 cm, with a sharp lower contact and a distinct and dispersed upward tail in shard concentrations, with a minor peak at 1778–1779 cm. Both of these deposits clearly occur within the MIS 5e plateau, which is an expanded section in core MD99-2253. Geochemical results from 1858 –1859 cm obtained by microprobe analysis reveal a homogenous rhyolitic glass population which is correlated to the widespread mid MIS 5e horizon (Fig. 11 and Supplementary information). This fine-grained glass deposit with a homogenous geochemical composition and no IRD signal supports deposition by primary tephra fall (Figs. 10 and 11). A sharp lower contact and distinct peak in shard concentration is a common feature of this deposit observed in other records (e.g. Wastegård and Rasmussen, 2001; Brendryen et al., 2010; Abbott et al., 2014).

The long declining tail in shard concentration above 1858–1859 cm is a typical feature of marine cryptotephra deposits and may well be indicative of the re-distribution of glass shards by ocean currents and upward mixing processes (Manville and Wilson, 2004; Lowe, 2011; Todd et al., 2014; Griggs et al., accepted). To test this, material from a minor peak of ~300 shards in this tail at 1778–1779 cm was additionally analysed (Fig. 10). This material was found to have a homogenous rhyolitic composition, but the composition showed that it was unrelated to the shards at 1858–1859 cm (Fig. 11). Although the volcanic source within Iceland is uncertain, we believe that this horizon represents a new, previously unknown volcanic event that may only be preserved in more westerly records within the North Atlantic. However, although this level represents the highest shard concentration between 1770 and 1820 cm, we believe that further geochemical analyses are required on samples between 1859 cm and 1779 cm in order to pinpoint the position of this isochron relative to the tail-off in shard concentrations above 1858–1859 cm. This contrasts with findings presented in Abbott et al. (2014) whereby material in two upward tails following major shard peaks was identical to the underlying peak and thus were most likely derived from secondary deposition and upward mixing. The results from MD99-2253 adds a further level of complexity to cryptotephra work but reinforces the importance of undertaking a systematic investigation of glass-shard concentrations to determine the peak shard position relative to background levels along with detailed geochemical analysis. Not only are steps of this kind important for defining the position of the isochron, but also for determining whether additional primary-deposited cryptotephras may be hidden within the long tail that usually follow the peak in shard concentration (e.g. Gehrels et al., 2006, 2008). In contrast, the distinct peak in basaltic material relative to the low-shard-count background (<50 shards) at 1798–1799 cm is a clear marker for the position of this tephra. Such distinct peaks are indicative of a rapid input of material and major element results indicate that this horizon is a homogenous tholeiitic basalt tephra sourced from Grimsvötn (Fig. 11). A few outliers of transitional alkali composition are observed, but the main population falls within the tholeiitic field. Again the geochemical characteristics, and lack of IRD signal, suggests that this horizon derives from a primary fall event, but no tephra with this glass geochemical signature and Eemian age has yet been reported. We believe that this deposit at 1798–1799 cm has potential as a tephra isochron and hence it is included within the marine tephra framework in Fig. 1.

In contrast to the Eemian tephras, ice-rafted deposits are identified in the uppermost interval investigated within MD99-2253. Two peaks in fine-grained brown glass shards are observed at 1542–1543 cm and 1586–1595 cm where higher concentrations of coarse-grained shards are also identified. Shards from 1542–1543 cm reveal a relatively homogenous basaltic tholeiitic composition typical of Grimsvötn-sourced material (but with wide-ranging CaO and TiO_2 values). In contrast, heterogenous geochemistry is a feature of glass shards extracted from sediment intervals between 1586–1595 cm with both tholeiitic and transitional alkali shards identified, spanning several different source compositional envelopes (Fig. 11). Both deposits coincide with peaks in IRD and hence, we believe that both are the result of ice-rafting. Their use as isochronous horizons, therefore, may be limited due to uncertainties in the delay associated with deposition in the marine realm. However, the higher degree of geochemical homogeneity within 1542–1543 cm may reflect only a short delay between the Grimsvötn eruption and associated deposition of tephra on ice and subsequent iceberg calving. It is possible that one of these deposits may correspond to the ice-berg-rafted 5c-DO24s/BAS-I and 5c-Midt/BAS-I horizons of similar age and geochemistry found within the Norwegian Sea and Faroes region (Brendryen et al., 2010; Abbott et al., 2014). However, further geochemical characterisations are required to assess whether indeed a firm and diagnostic correlation can be made. This possible correlation indicates some promise in utilising 5c-DO24s/BAS-I as a regional stratigraphic marker within the marine realm, but the potential delay in deposition may limit its wider application.

Thus, an assessment of several different lines of evidence is essential and very valuable to ensure the correct utilisation of marine cryptotephra deposits as isochronous marker horizons. It is clear that glass shard concentration profiles, grain-size distribution, and geochemical analysis of multiple shards along with an associated IRD record are essential indicators for these purposes. Further details on assessing the integrity of marine tephra deposits is provided by Griggs et al. (2014) along with the novel use of micromorphological techniques to investigate the deposition of tephras in ocean sediments.

3. Marine-based correlations: the potential and challenges ahead

Several of the cryptotephras outlined in the tephrostratigraphical framework for 130–60 ka b2k have clear potential to act as pivotal isochronous markers between sequences. We expect that, with time, there will be new additions and refinements, but the synthesis presented in Fig. 1 provides a valuable starting point for establishing key time-lines between records. For the younger INTIMATE tephra framework (60–8 ka b2k), Davies et al. (2012) highlighted the key tephras from that interval that were considered as being most valuable for correlative purposes, according to their spatial distribution, diagnostic geochemical signature, well-constrained age-estimate and association with rapid climatic events. For the 130–60 ka b2k time-interval, we feel that it is premature to pinpoint the most valuable isochrons according to these criteria. Several of the tephras represent single occurrences and, with just a handful of reported cryptotephra studies, the full spatial distribution remains to be deciphered. Nonetheless, we are able to suggest which cryptotephras hold the greatest potential for

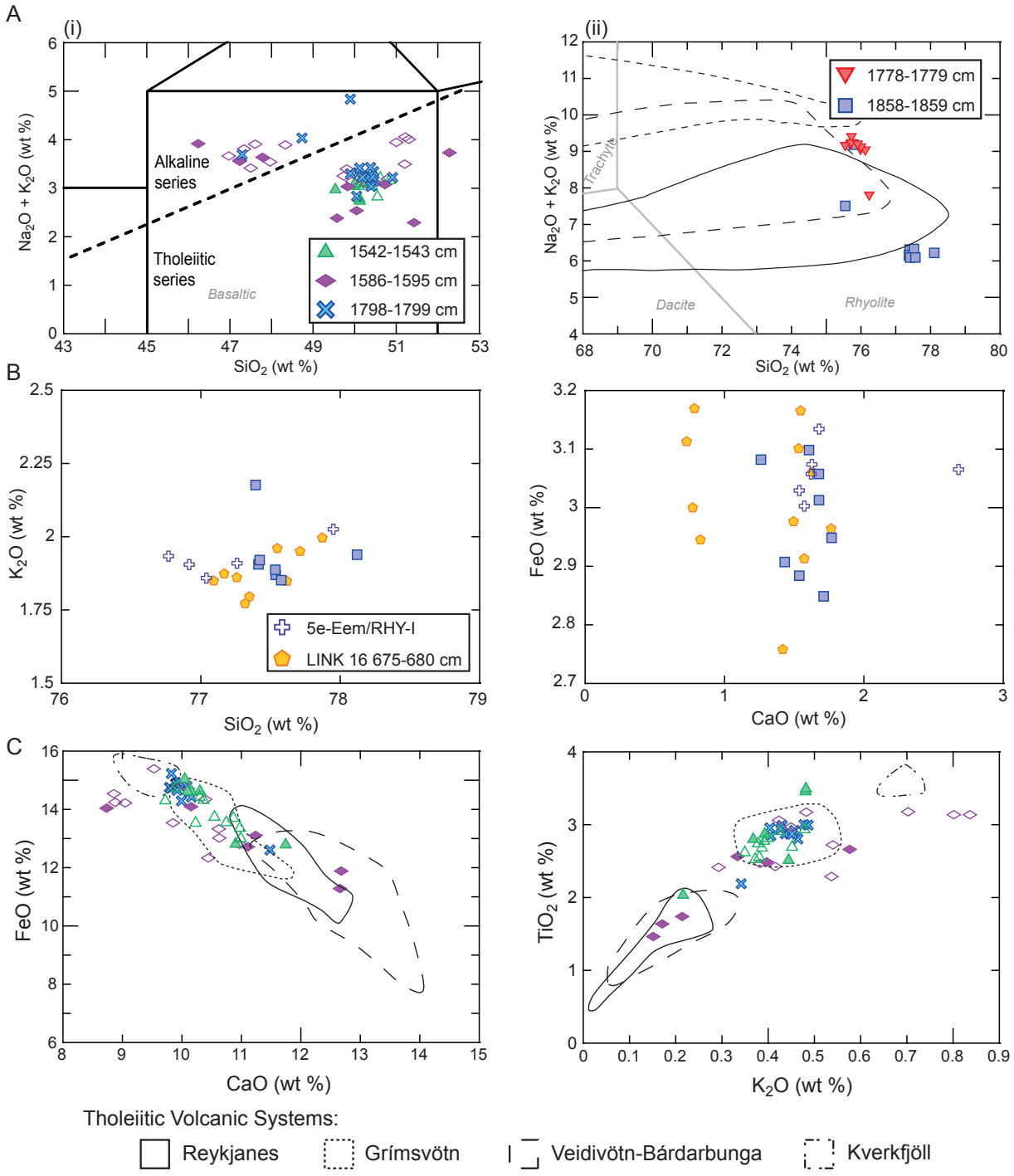

Fig. 11. Major element results for analyses of glass from five tephras found in MD99-2253. A: Geochemical classification on the total alkali silica plot for (i) the basaltic tephras 1542–1543 cm, 1586–1595 cm, 1798–1799 cm; and (ii) the rhyolitic tephras 1778–1779 cm and 1858–1859 cm. B: SiO_2 vs K_2O and CaO vs FeO biplots for the tephra at 1858–1859 cm. 5e-Eem-RHY-I from Brendryen et al. (2010) and LINK 16 675–680 cm (also correlated to 5e-Eem-RHY-I) from Abbott et al. (2014) are also shown. C: CaO vs FeO and K_2O vs TiO_2 biplots for analyses of glass from the basaltic tephras alongside the geochemical envelopes for glass analyses from tholeiitic volcanic systems using data presented in Jakobsson (1979), Haflidason et al. (2000), Jakobsson et al. (2008), and Höskuldsson et al. (2006). All data are normalised, total Fe is reported as FeO and the full data-set is available in the Supplementary information. In A and C open symbols represent glass shard extracted from the 25–80 μm fraction and closed symbols represent shards that are >80 μm.

precisely correlating different proxy records and those that will aid in testing the key climatic questions. For instance, NGRIP 2548.35 m, NGRIP 2903.85 m, and NGRIP 2953.35 m were deposited close to sharp cooling transitions, NGRIP 2574.55 m, NGRIP 2745.60, and 2742.85 m lie close to signals of rapid warmings, and the couplet NGRIP 2607.95 m and NGRIP 2600.60 m are associated with a short-lived climatic oscillation. If these nine cryptotephras can be traced in the marine environment, they hold considerable promise for precisely constraining the sequential changes associated with a rapid climatic event. As yet, very few marine cores have been investigated for their cryptotephra record and several sampling gaps still remain within the ice-core records. Thus, advancing

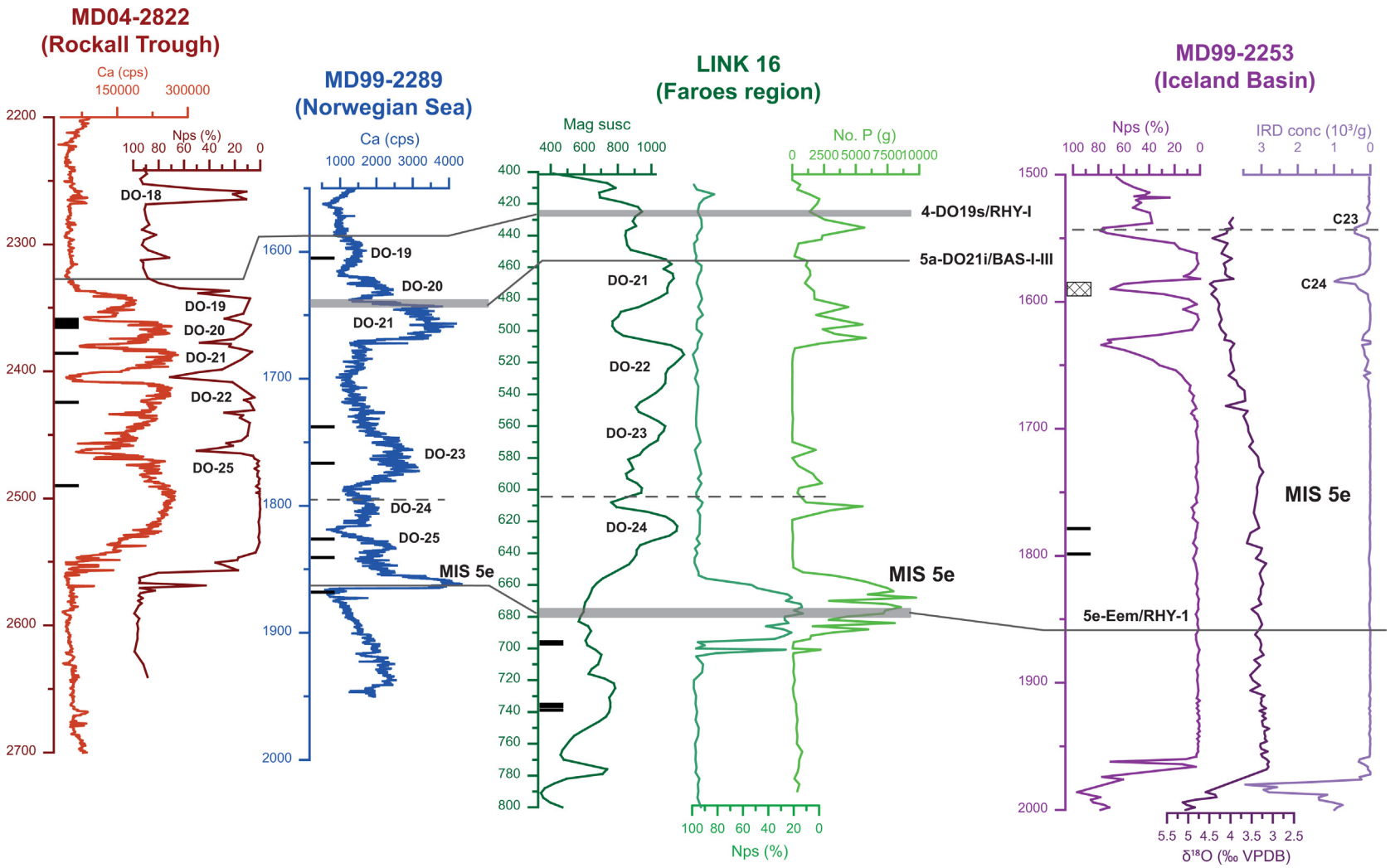

Fig. 12. Tephra-based marine correlation of MD04-2822 (Hibbert et al., 2010), MD99-2289 (Brendryen et al., 2010; Abbott et al., 2014; Rasmussen, T. unpublished), LINK 16 (Abbott et al., 2014; Rasmussen, T. unpublished), and MD99-2253. Each record is plotted on a depth scale (cm). The following proxies are shown: bulk sediment calcium record (counts per second) analysed by XRF, percentage abundance of *Neogloboquadrina pachyderma (s)* (Nps %), magnetic susceptibility (mag susc), number of planktonic foraminifera per gram sediment dry weight (No. P (g)), oxygen isotopes record ($\delta^{18}O$ ‰ relative to the VPDB standard) measured using the benthic foraminifer *Cibicidoides wuellerstorfi* in core MD99-2253 and ice-rafted detrital concentrations (IRD $\times 10^3$per g). Three tephra deposits are traced between these core records (grey lines): 5e-Eem/RHY-I, 5a-DO21i/BAS I-III, and 4-DO19s/RHY-I. 5a-DO21i/BAS I-III is thought to represent three distinct separate tephra horizons that are geochemically indistinguishable from one another and the LINK 16 675-80 cm deposit is correlated to all three events (Abbott et al., 2014) (hence the thicker line in MD99-2289). The stratigraphic positions of other tephras identified in each record are represented by black bars adjacent to the depth scale. The thickness of these black bars and the grey lines define the full stratigraphic extent of the tephra according to the shard concentration profiles. Also shown for reference is the position of the 5c-DO24s/BAS-I tephra (grey dotted line). Sub-populations of this deposit are found in MD99-2289, LINK 16, and MD99-2253, although its use as an isochronous marker horizon is limited by the potential lag in deposition because of ice-berg rafting. Hatched bar in MD99-2253 represents an ice-berg rafted deposit. Dansgaard–Oeschger (DO) events are marked according to the recommendations of (Rasmussen et al., 2014) and are thought to represent correlative Greenland Interstadial (GI) events in the Greenland ice-cores.

this approach requires a concerted effort to reconstruct the full tephra distribution and dispersal pathways in the North Atlantic region. Although basaltic tephras dominate the ice-core record, the individual tephra signatures do form distinct geochemical populations that are well-constrained stratigraphically against the NGRIP oxygen isotope record (Figs. 1 and 4). The results from this time-interval indicate that there are no closely-timed tephras of similar geochemical composition (cf. Bourne et al., 2013). The only exceptions are NGRIP 2944.90 m and NGRIP 2953.35 m separated by ca. 1330 years – both of which are basaltic transitional alkali and occupy similar, but not identical, fields on glass-based geochemical biplots (Fig. 4).

In the marine realm, the most widespread isochrons (e.g. 5e-Eem/RHY-1 and 4-DO19s/RHY-I) provide key tie-points for comparing palaeoclimatic signals in a time period where independent chronological controls are rare and where chronological models are largely constructed by direct synchronisation to the Greenland ice-cores, marine $\delta^{18}O$ stratigraphies or both (e.g. Hibbert et al., 2010). What can be achieved when tephras or cryptotephras of identical glass geochemical composition can be detected in disparate records is demonstrated in Fig. 12. Three tephras have been traced in marine cores from the Rockall Trough, Norwegian Sea, Faroes region, and Iceland Basin and provide the means to precisely correlate these records and piece together a reconstruction of changes in the marine realm. We present the proxy data available for these different records, and the correlations permitted using the 5e-Eem/RHY-I and 4-DO19s/RHY-I tephras support synchronous changes within the marine realm during two contrasting climatic episodes. Tephra 5e-Eem/RHY-I fell at the peak warmth of the Eemian period in both the Faroes region, Norwegian Sea, and Iceland Basin as demonstrated by the low percentage abundance of the polar planktonic foraminiferal species *Neogloboquadrina pachyderma (s)* and bulk sediment Ca content (Fig. 12). This is also consistent with the results reported by Wastegård et al. (2005) of the position of this tephra within a terrestrial sequence on the Faroe Islands, although they concluded that the Eemian optimum in this region lagged behind that experienced in continental Europe.

In contrast to the 5e-Eem/RHY-I tephra, the 4-DO19s/RHY-I tephra was deposited during a cold episode shortly after a sharp cooling transition thought to be correlative to GI-19 event in the ice-cores. This cooling transition is marked by a decline in the number of planktonic foraminifera in the Faroes core, an abrupt increase in the *N. pachyderma (s)* abundances and the bulk sediment calcium content from the Rockall Trough, and a fall in the Ca content in the Norwegian Sea sediments (Fig. 12). The stratigraphic positions of both the 5e-Eem/RHY-I tephra and the 4-DO19s/RHY-I tephras supports the notion of synchronous changes in the oceans but an insight into the phasing associated with abrupt events is not possible because of the timing of these events during relatively stable climatic conditions or just after a rapid transition. Tephra from 5a-DO21i/BAS I-III, spans the cooling transition of Dansgaard–Oeschger (DO)-21 identified in the Ca content of MD99-2289 (Fig. 12), however, this transition is not so well-defined in the number of planktonic foraminifera in LINK16 but a fall is evident in the magnetic susceptibility record after tephra deposition. Because the magnetic susceptibility record is smoothed, further work is required to define this cooling transition and to employ this tephra as a correlative marker for assessing the climatic phase relationships associated with this transition. However, despite the valuable stratigraphic position, this tephra deposit lacks a distinct diagnostic geochemical signature as it seems that several tephras with Grimsvötn-type chemistry were erupted during this interval (see above and Fig. 9). Thus the most valuable isochrons will need to meet all key criteria to fulfil a pivotal role for testing the phasing relationships between the atmospheric and oceanic systems.

4. Conclusions

The framework presented here represents an essential first-step for advancing the potential and application of tephrochronology between 130 and 60 ka b2k, akin to the developments experienced within the succeeding INTIMATE time-frame. This emerging framework forms a basis for the identification of coeval tephra and cryptotephra deposits in other depositional archives spanning this time-interval and, as demonstrated for the marine environment, has the potential to provide an underpinning structure for geochronological models, obviating the propensity to simply align and synchronise records at rapid climatic transitions (Fig. 12) (e.g. Austin and Hibbert, 2012; Blaauw, 2012). Prior to meeting this potential, several challenges require attention. Firstly, a step-change is required to search for cryptotephras in high sedimentation and more distal areas of the North Atlantic region, where some of the cryptotephras recorded in NGRIP may also be preserved as discrete deposits. Work of this kind requires systematic down-core searches to determine glass-shard concentration profiles, detailed geochemical analyses of multiple shards to assess the homogeneity of a cryptotephra horizon along with an assessment of any coeval input of ice-rafted material. It is also clear that a narrow targeted sampling approach that solely focuses on large sulphate peaks in the ice is ineffective for tracing a comprehensive record of cryptotephras. Furthermore, robust geochemical fingerprinting is particularly crucial to the success of this approach. With several basaltic tholeiitic horizons identified in the ice and marine cores, tephra-based correlations between cores will depend on subtle but diagnostic features of glass (Brendryen et al., 2010; Bourne et al., 2013, 2014; Rasmussen et al., 2013; Seierstad et al., 2014). Subtleties of this kind are often only robustly characterised by “side by side” microprobe analysis of potential correlative deposits (Lowe, 2011; Bourne et al., 2013; Abbott et al., 2014).

Ultimately, this framework and recommendations for further work provide the basis to widen the tephra-based correlations beyond the marine environment to the ice-core realm and potentially to the handful of terrestrial sequences and ‘snapshots’ that preserve climatic changes during this time-interval (Helmens et al., 2007). Undoubtedly, tephrochronology represents a powerful approach that has the potential to test the degree of synchroneity between atmospheric, marine and terrestrial proxies over rapid climatic transitions of the last interglacial/glacial period – a key step towards testing the climatic-forcing mechanisms.

Acknowledgements

The new results presented here have been supported by NERC funding (NE/FE020600/1, NE/F02116X/1, NE/F021445/1, NE/G005230/1). The overall synthesis and review of published data represents the culmination of several years work and support from NERC: NE/D00416/1, NER/S/A/2995/13417, the European Research Council (TRACE project) under the European Union’s Seventh Framework Programme(FP7/2007-2013) / ERC grant agreement no. [259253] and EU-COST ACTION INTIMATE (ESO907) (http://cost-es0907.geoenvi.org/). Gareth James, Anna Bourne, Eliza Cook, Inger Seierstad and Lars Berg Larsen are acknowledged for laboratory assistance and ice-core sampling at the University of Copenhagen. Anna Ratcliffe assisted in editing and improving Figs. 1, 4 and 8. We also thank Stefan Wastegård, JP Steffensen and Jo Brendryen for fruitful discussion over a number of years. Chris Hayward provided essential support during the electron microprobe work at the University of Edinburgh. SMD, PMA, RhHM and NJGP also acknowledge the support of the Climate

Change Consortium of Wales (C3W). This work is also a contribution to the NorthGRIP ice-core project, which is directed and organised by the Centre for Ice and Climate at the Niels Bohr Institute, University of Copenhagen. It is being supported by funding agencies in Denmark (SNF), Belgium (FNRSCFB), France (IFRTP and INSU/CNRS), Germany (AWI), Iceland (RannIs), Japan (MEXT), Sweden (SPRS), Switzerland (SNF) and the United States of America (NSF). We are also grateful to David Lowe and Sabine Wulf for their thorough and constructive reviews.

Appendix A. Supplementary data

Supplementary data related to this article can be found at http://dx.doi.org/10.1016/j.quascirev.2014.03.024.

References

Abbott, P.M., Austin, W.E.N., Davies, S.M., Pearce, N.J.G., Hibbert, F.D., 2013. Cryptotephrochronology of the Eemian and the last interglacial-glacial transition in the North East Atlantic. J. Quat. Sci. 28, 501–514.

Abbott, P.M., Austin, W.E.N., Davies, S.M., Pearce, N.J.G., Rasmussen, T.L., Wastegård, S., 2014. Re-evaluation and extension of the Marine Isotope Stage 5 tephrostratigraphy of the Faroe Islands Region: the cryptotephra record. Palaeogeography, Palaeoclimatology, Palaeoecology 409, 153–168.

Abbott, P.M., Davies, S.M., 2012. Volcanism and the Greenland ice-cores: the tephra record. Earth-Sci Rev. 115, 173–191.

Abbott, P.M., Davies, S.M., Austin, W.E.N., Pearce, N.J.G., Hibbert, F.D., 2011. Identification of cryptotephra horizons in a North East Atlantic marine record spanning marine isotope stages 4 and 5a (similar to 60,000-82,000 a b2k). Quat. Int. 246, 177–189.

Abbott, P.M., Davies, S.M., Steffensen, J.P., Pearce, N.J.G., Bigler, M., Johnsen, S.J., Seierstad, I.K., Svensson, A., Wastegard, S., 2012. A detailed framework of Marine Isotope Stages 4 and 5 volcanic events recorded in two Greenland ice-cores. Quat. Sci. Rev. 36, 59–77.

Andrews, J.T., Geirsdóttir, A., Hardardóttir, J., Principato, S., Grönvold, K., Kristjansdóttir, G.B., Helgadóttir, G., Drexler, J., Sveinbjörnsdóttir, A., 2002. Distribution, sediment magnetism and geochemistry of the Saksunarvatn (10 180 ± 60 cal. yr BP) tephra in marine, lake, and terrestrial sediments, northwest Iceland. J. Quat. Sci. 17, 731–745.

Austin, W.E.N., Hibbert, F.D., 2012. Tracing time in the ocean: a brief review of chronological constraints (60-8 kyr) on North Atlantic marine event-based stratigraphies. Quat. Sci. Rev. 36, 28–37.

Austin, W.E.N., Hibbert, F.D., Rasmussen, S.O., Peters, C., Abbott, P.M., Bryant, C.L., 2012. The synchronization of palaeoclimatic events in the North Atlantic region during Greenland Stadial 3 (ca 27.5 to 23.3 kyr b2k). Quat. Sci. Rev. 36, 154–163.

Austin, W.E.N., Wilson, L.J., Hunt, J.B., 2004. The age and chronostratigraphical significance of North Atlantic Ash Zone II. J. Quat. Sci. 19, 137–146.

Bigler, M., 2004. Hochauflö sende Spurenstoffmessungen an polaren Eisbohrkernen: Glazio-chemische und klimatische Prozessstudien. University of Bern, Switzerland.

Blaauw, M., 2012. Out of tune: the dangers of aligning proxy archives. Quat. Sci. Rev. 36, 38–49.

Blockley, S.P.E., Lane, C.S., Hardiman, M., Rasmussen, S.O., Seierstad, I.K., Steffensen, J.P., Svensson, A., Lotter, A.F., Turney, C.S.M., Ramsey, C.B., INTIMATE group, 2012. Synchronisation of palaeoenvironmental records over the last 60,000 years, and an extended INTIMATE(1) event stratigraphy to 48,000 b2k. Quat. Sci. Rev. 36, 2–10.

Blockley, S.P.E., Brauer, A., Davies, S.M., Hardiman, M., Harding, P., Lane, C.S., MacLeod, A., Matthews, I., Pyne-O'Donnell, S., Rasmussen, S.O., Wulf, S., G., Zanchetta., 2014. Tephrochronology and the extended INTIMATE (Integration of Ice-core, Marine and Terrestrial records) event stratigraphy 8–128 ka b2k. Quat. Sci. Rev. 106, 88–100.

Boch, R., Cheng, H., Spötl, C., Edwards, R.L., Wang, X., Häuselmann, P., 2011. NALPS: a precisely dated European climate record 120–60 ka. Clim. Past 7, 1247–1259.

Bourne, A.J., Davies, S.M., Abbott, P.M., Rasmussen, S.O., Steffensen, J.P., Svensson, A., 2013. Revisiting the Faroe Marine Ash Zone III in two Greenland ice cores: implications for marine-ice correlations. J. Quat. Sci. 28, 641–646.

Bourne, A.J., Cook, E., Abbott, P.M., Seierstad, I.K., Steffensen, J-P., Svensson, A., Schüpbach, S., Fischer, H., Davies, S.M., 2014. A tephra lattice for Greenland and a reconstruction of volcanic events spanning 25–45 ka b2k. Quat. Sci. Rev. (in press).

Boygle, J.E., 1994. Tephra in Lake Sediments: an Unambiguous Geochronological Marker? University of Edinburgh, Edinburgh.

Brendryen, J., Haflidason, H., Sejrup, H.P., 2010. Norwegian Sea tephrostratigraphy of marine isotope stages 4 and 5: prospects and problems for tephrochronology in the North Atlantic region. Quat. Sci. Rev. 29, 847–864.

Cannariato, K.G., Kennett, J.P., 2005. Structure of the penultimate deglaciation along the California margin and implications for Milankovitch theory. Geology 33, 157–160.

Capron, E., Landais, A., Chappellaz, J., Schilt, A., Buiron, D., Dahl-Jensen, D., Johnsen, S.J., Jouzel, J., Lemieux-Dudon, B., Loulergue, L., Leuenberger, M., Masson-Delmotte, V., Meyer, H., Oerter, H., Stenni, B., 2010. Millennial and sub-millennial scale climatic variations recorded in polar ice cores over the Last Glacial period. Clim. Past 6, 345–365.

Chapman, M.R., Shackleton, N.J., 1999. Global ice-volume fluctuations, North Atlantic ice-rafting events, and deep-ocean circulation changes between 130 and 70 ka. Geology 27, 795–798.

Coulter, S.E., Pilcher, J.R., Plunkett, G., Baillie, M., Hall, V.A., Steffensen, J.P., Vinther, B.M., Clausen, H.B., Johnsen, S.J., 2012. Holocene tephras highlight complexity of volcanic signals in Greenland ice cores. J. Geophys. Res. Atmos. 117.

Dahl-Jensen, D., Albert, M.R., Aldahan, A., Azuma, N., Balslev-Clausen, D., Baumgartner, M., Berggren, A.M., Bigler, M., Binder, T., Blunier, T., Bourgeois, J.C., Brook, E.J., Buchardt, S.L., Buizert, C., Capron, E., Chappellaz, J., Chung, J., Clausen, H.B., Cvijanovic, I., Davies, S.M., Ditlevsen, P., Eicher, O., Fischer, H., Fisher, D.A., Fleet, L.G., Gfeller, G., Gkinis, V., Gogineni, S., Goto-Azuma, K., Grinsted, A., Gudlaugsdottir, H., Guillevic, M., Hansen, S.B., Hansson, M., Hirabayashi, M., Hong, S., Hur, S.D., Huybrechts, P., Hvidberg, C.S., Iizuka, Y., Jenk, T., Johnsen, S.J., Jones, T.R., Jouzel, J., Karlsson, N.B., Kawamura, K., Keegan, K., Kettner, E., Kipfstuhl, S., Kjaer, H.A., Koutnik, M., Kuramoto, T., Kohler, P., Laepple, T., Landais, A., Langen, P.L., Larsen, L.B., Leuenberger, D., Leuenberger, M., Leuschen, C., Li, J., Lipenkov, V., Martinerie, P., Maselli, O.J., Masson-Delmotte, V., McConnell, J.R., Miller, H., Mini, O., Miyamoto, A., Montagnat-Rentier, M., Mulvaney, R., Muscheler, R., Orsi, A.J., Paden, J., Panton, C., Pattyn, F., Petit, J.R., Pol, K., Popp, T., Possnert, G., Prie, F., Prokopiou, M., Quiquet, A., Rasmussen, S.O., Raynaud, D., Ren, J., Reutenauer, C., Ritz, C., Rockmann, T., Rosen, J.L., Rubino, M., Rybak, O., Samyn, D., Sapart, C.J., Schilt, A., Schmidt, A.M.Z., Schwander, J., Schupbach, S., Seierstad, I., Severinghaus, J.P., Sheldon, S., Simonsen, S.B., Sjolte, J., Solgaard, A.M., Sowers, T., Sperlich, P., Steen-Larsen, H.C., Steffen, K., Steffensen, J.P., Steinhage, D., Stocker, T.F., Stowasser, C., Sturevik, A.S., Sturges, W.T., Sveinbjornsdottir, A., Svensson, A., Tison, J.L., Uetake, J., Vallelonga, P., van de Wal, R.S.W., van der Wel, G., Vaughn, B.H., Vinther, B., Waddington, E., Wegner, A., Weikusat, I., White, J.W.C., Wilhelms, F., Winstrup, M., Witrant, E., Wolff, E.W., Xiao, C., Zheng, J., Community, N., 2013. Eemian Interglacial reconstructed from a Greenland folded ice core. Nature 493, 489–494.

Davies, S.M., Abbott, P.M., Pearce, N.J.G., Wastegard, S., Blockley, S.P.E., 2012. Integrating the INTIMATE records using tephrochronology: rising to the challenge. Quat. Sci. Rev. 36, 11–27.

Davies, S.M., Turney, C.S.M., Lowe, J.J., 2001. Identification and significance of a visible, basalt-rich Vedde Ash layer in a Late-Glacial sequence on the Isle of Skye, Inner Hebrides, Scotland. J. Quat. Sci. 16, 99–104.

Davies, S.M., Wastegard, S., Abbott, P.M., Barbante, C., Bigler, M., Johnsen, S.J., Rasmussen, T.L., Steffensen, J.P., Svensson, A., 2010. Tracing volcanic events in the NGRIP ice-core and synchronising North Atlantic marine records during the Last Glacial period. Earth Planet. Sci. Lett. 294, 69–79.

Davies, S.M., Wastegård, S., Rasmussen, T.L., Svensson, A., Johnsen, S.J., Steffensen, J.P., Andersen, K.K., 2008. Identification of the Fugloyarbanki tephra in the NGRIP ice core: a key tie-point for marine and ice-core sequences during the Last Glacial period. J. Quat. Sci. 23, 409–414.

Dugmore, A.J., Newton, A.J., 1998. Holocene tephra layers in the Faroe Islands. Frodskaparrit 46, 191–204.

Fiacco, R.J., Palais, J.M., Germani, M.S., Zielinski, G.A., Mayewski, P.A., 1993. Characteristics and possible source of a 1479 A.D. Volcanic ash layer in a Greenland ice core. Quat. Res. 39, 267–273.

Fiacco, R.J., Thordarson, T., Germani, M.S., Self, S., Palais, J.M., Whitlow, S., Grootes, P.M., 1994. Atmospheric aerosol loading and transport due to the 1783-84 Laki eruption in Iceland, interpreted from ash particles and acidity in the GISP2 ice core. Quat. Res. 42, 231–240.

Fleitmann, D., Cheng, H., Badertscher, S., Edwards, R.L., Mudelsee, M., Göktürk, O.M., Fankhauser, A., Pickering, R., Raible, C.C., Matter, A., Kramers, J., Tüysüz, O., 2009. Timing and climatic impact of Greenland interstadials recorded in stalagmites from northern Turkey. Geophys. Res. Lett. 36, L19707.

Fronval, T., Jansen, E., Haflidason, H., Sejrup, J.P., 1998. Variability in surface and deep water conditions in the Nordic seas during the Last Interglacial period. Quat. Sci. Rev. 17, 963–985.

Galaasen, E.V., Ninnemann, U.S., Irvali, N., Kleiven, H.F., Rosenthal, Y., Kissel, C., Hodell, D.A., 2014. Rapid reductions in North Atlantic deep water during the peak of the Last Interglacial period. Science 343, 1129–1132.

Gao, C., Robock, A., Ammann, C., 2008. Volcanic forcing of climate over the past 1500 years: an improved ice core-based index for climate models. J. Geophys. Res. Atmos. 113, D23111.

Gehrels, M.J., Lowe, D.J., Hazell, Z.J., Newnham, R.M., 2006. A continuous 5300-yr Holocene cryptotephrostratigraphic record from northern New Zealand and implications for tephrochronology and volcanic hazard assessment (vol. 16, pg 173, 2006). Holocene 16, 624.

Gehrels, M.J., Newnham, R.M., Lowe, D.J., Wynne, S., Hazell, Z.J., Caseldine, C., 2008. Towards rapid assay of cryptotephra in peat cores: review and evaluation of various methods. Quat. Int. 178, 68–84.

Griggs, A.J., Davies, S.M., Abbott, P.M., Rasmussen, T.L., Palmer, A.P., 2014. Optimising the use of marine tephrochronology in the North Atlantic: a detailed investigation of the Faroe Marine Ash Zones II, III and IV. Quat. Sci. Rev. 106, 122–139.

Grönvold, K., Oskarsson, N., Johnsen, S.J., Clausen, H.B., Hammer, C.U., Bond, G., Bard, E., 1995. Ash layers from Iceland in the GRIP ice core correlated with oceanic and land sediments. Earth Planet. Sci. Lett. 135, 149–155.

Haflidason, H., Eiríksson, J., van Kreveld, S., 2000. The tephrochronology of Iceland and the North Atlantic region during the Middle and Late Quaternary: a review. J. Quat. Sci. 15, 3–22.
Hayward, C., 2012. High spatial resolution electron probe microanalysis of tephras and melt inclusions without beam-induced chemical modification. Holocene 22, 119–125.
Helmens, K.F., Bos, J.A.A., Engels, S., Van Meerbeeck, C.J., Bohncke, S.J.P., Renssen, H., Heiri, O., Brooks, S.J., Seppa, H., Birks, H.J.B., Wohlfarth, B., 2007. Present-day temperatures in northern Scandinavia during the last glaciation. Geology 35, 987–990.
Heuser, L., Oppo, D., 2003. Millennial- and orbital-scale climate variability in southeastern United States and in the subtropical Atlantic during Marine Isotope Stage 5: evidence from pollen and isotopes in ODP Site 1059. Earth Planet. Sci. Lett. 214, 483–490.
Hibbert, F.D., Austin, W.E.N., Lenc, M.J., Gatliff, R.W., 2010. British Ice Sheet dynamics inferred from North Atlantic ice-rafted debris records spanning the last 175 000 years. J. Quat. Sci. 25, 461–482.
Höskuldsson, Á., Sparks, R.S.J., Carroll, M.R., 2006. Constraints on the dynamics of subglacial basalt eruptions from geological and geochemical observations at Kverkfjöll, NE-Iceland. Bull. Volcanol. 68, 689–701.
Hunt, J.B., Fannin, N.G.T., Hill, P.G., Peacock, J.D., 1995. The tephrochronology and radiocarbon dating of North Atlantic, Late Quaternary sediments: an example from the St Kilda Basin. In: Scrutton, R.A., Stoker, M.S., Shimmield, G.B., Tudhope, A.W. (Eds.), The Tectonics, Sedimentation and Palaeoceanography of the North Atlantic Region, pp. 227–248. London.
Jakobsson, S.P., 1979. Outline of the petrology of Iceland. Jökull 29, 57–73.
Jakobsson, S.P., Jónasson, K., Sigurdsson, I.A., 2008. The three igneous rock suites of Iceland. Jökull 58, 117–138.
Knudsen, K.-L., Seidenkrantz, M.-S., Kristensen, P., 2002. Last interglacial and early glacial circulation in the Northern North Atlantic Ocean. Quat. Res. 58, 22–26.
Kuhs, M., Austin, W.E.N., Abbott, P.M., Hodell, D.A., 2014. Iceberg-rafted tephra as a potential tool for the reconstruction of ice-sheet processes and ocean surface circulation in the glacial North Atlantic. In: Austin, W.E.N., Abbott, P.M., Davies, S.M., Pearce, N.J.G., Wastegård, S. (Eds.), Marine Tephrochronology, Geological Society, London, Special Publications, 398.
Lacasse, C., Carey, S., Sigurdsson, H., 1998. Volcanogenic sedimentation in the Iceland Basin: influence of subaerial and subglacial eruptions. J. Volcanol. Geotherm. Res. 83, 47–73.
Lacasse, C., Garbe-Schönberg, C.-D., 2001. Explosive silicic volcanism in Iceland and the Jan Mayen area during the last 6 Ma: sources and timing of major eruptions. J. Volcanol. Geotherm. Res. 107, 113–147.
Lane, C.S., Andrič, M., Cullen, V.L., Blockley, S.P.E., 2011. The occurrence of distal Icelandic and Italian tephra in the Lateglacial of Lake Bled. Quat. Sci. Rev. 30, 1013–1018.
Lane, C.S., Brauer, A., Blockley, S.P.E., Dulski, P., 2013. Volcanic ash reveals time-transgressive abrupt climate change during the Younger Dryas. Geology. 41, 1251–1254.
Larsen, G., Eiríksson, J., Knudsen, K.-L., Heinemeier, J., 2002. Correlation of Late Holocene terrestrial and marine tephra markers, north Iceland: implications for reservoir age changes. Polar Res. 21, 283–290.
Le Maitre, R.W., 1989. A Classification of Igneous Rocks and Glossary of Terms. Blackwell Scientific Publications.
Lehman, S.J., Sachs, J.P., Crotwell, A.M., Keigwin, L.D., Boyle, E.A., 2002. Relation of subtropical Atlantic temperature, high-latitude ice rafting, deep water formation, and European climate 130,000-60,000 years ago. Quat. Sci. Rev. 21, 1917–1924.
Lisiecki, L.E., Raymo, M.E., 2005. A Pliocene-Pleistocene stack of 57 globally distributed benthic delta O-18 records (vol. 20, art no PA1003, 2005). Paleoceanography 20.
Lototskaya, A., Ganssen, G.M., 1999. The structure of termination II (penultimate deglaciation and Eemian) in the North Atlantic. Quat. Sci. Rev. 18, 1641–1654.
Lowe, D.J., 2011. Tephrochronology and its application: a review. Quat. Geochronol. 6, 107–153.
Lowe, J.J., Hoek, W.Z., INTIMATE group, 2001. Inter-regional correlation of palaeoclimatic records for the Last Glacial-Interglacial transition: a protocol for improved precision recommended by the INTIMATE project group. Quat. Sci. Rev. 20, 1175–1187.
Lowe, J.J., Rasmussen, S.O., Björck, S., Hoek, W.Z., Steffensen, J.P., Walker, M.J.C., Yu, Z.C., 2008. Synchronisation of palaeoenvironmental events in the North Atlantic region during the Last Termination: a revised protocol recommended by the INTIMATE group. Quat. Sci. Rev. 27, 6–17.
Manville, V., Wilson, C.J.N., 2004. Vertical density currents: a review of their potential role in the deposition and interpretation of deep-sea ash layers. J. Geol. Soc. 161, 947–958.
McManus, J.F., Bond, G.C., Broecker, W.S., Johnsen, S.J., Labeyrie, L., Higgins, S., 1994. High-resolution climate records from the North Atlantic during the last interglacial. Nature 371, 326–329.
McManus, J.F., Oppo, D.W., Cullen, J.L., 1999. A 0.5-million- year record of millennial-scale climate variability in the North Atlantic Ocean. Science 283, 971–975.
McManus, J.F., Oppo, D.W., Keigwin, L.D., Cullen, J.L., Bond, G.C., 2002. Thermohaline circulation and prolonged interglacial warmth in the North Atlantic. Quat. Res. 58, 17–21.
Meyer, P.S., Sigurdsson, H., Schilling, J.G., 1985. Petrological and Geochemical variations along Iceland Neovolcanic zones. J. Geophys. Res. Solid 90, 43–72.
Mortensen, A.K., Bigler, M., Grönvold, K., Steffensen, J.P., Johnsen, S.J., 2005. Volcanic ash layers from the Last Glacial termination in the NGRIP ice core. J. Quat. Sci. 20, 209–219.
NGRIP members, 2004. High-resolution record of Northern Hemisphere climate extending into the last interglacial period. Nature 431, 147–151.
Óladottir, B.A., Sigmarsson, O., Larsen, G., Devidal, J.L., 2011. Provenance of basaltic tephra from Vatnajökull subglacial volcanoes, Iceland, as determined by major- and trace-element analyses. Holocene 21, 1037–1048.
Óladóttir, B.A., Sigmarsson, O., Larsen, G., Thordarson, T., 2008. Katla volcano, Iceland: magma composition, dynamics and eruption frequency as recorded by Holocene tephra layers. Bull. Volcanol. 70, 475–493.
Oppo, D.W., Keigwin, L.D., McManus, J.F., Cullen, J.L., 2001. Persistent suborbital climate variability in marine isotope stage 5 and Termination II. Paleoceanography 16, 280–292.
Palais, J.M., Kyle, P.R., 1988. Chemical-composition of ice containing tephra layers in the Byrd-Station Ice Core, Antarctica. Quat. Res. 30, 315–330.
Parrenin, F., Petit, J.R., Masson-Delmotte, V., Wolff, E., Basile-Doelsch, I., Jouzel, J., Lipenkov, V., Rasmussen, S.O., Schwander, J., Severi, M., Udisti, R., Veres, D., Vinther, B.M., 2012. Volcanic synchronisation between the EPICA Dome C and Vostok ice cores (Antarctica) 0–145 kyr BP. Clim. Past 8, 1031–1045.
Pearce, N.J.G., Abbott, P.M., Martin-Jones, C., 2014. Microbeam methods for the analysis of glass in fine grained tephra deposits: a SMART perspective on current and future trends. In: Austin, W.E.N., Abbott, P.M., Davies, S.M., Pearce, N.J.G., Wastegård, S. (Eds.), Marine Tephrochronology, Geological Society of London Special Publication, 398.
Pearce, N.J.G., Perkins, W.T., Westgate, J.A., Wade, S.C., 2011. Trace-element microanalysis by LA-ICP-MS: the quest for comprehensive chemical characterisation of single, sub-10 μm volcanic glass shards. Quat. Int. 246, 57–81.
Peters, C., Austin, W.E.N., Walden, J., Hibbert, F.D., 2010. Magnetic characterisation and correlation of a Younger Dryas tephra in North Atlantic marine sediments. J. Quat. Sci. 25, 339–347.
Rasmussen, S.O., Abbott, P.M., Blunier, T., Bourne, A.J., Brook, E.J., Buchardt, S.L., Buizert, C., Chappellaz, J., Clausen, H.B., Cook, E., Dahl-Jensen, D., Davies, S.M., Guillevic, M., Kipfstuhl, S., Laepple, T., Seierstad, I., Severinghaus, J.P., Steffensen, J.P., Stowasser, C., Svensson, A., Vallelonga, P., Vinther, B.M., Willhelms, F., Winstrup, M., 2013. A first chronology for the North Greenland Eemian Ice drilling ice core. Clim. Past 9, 2713–2730.
Rasmussen, S.O., Bigler, M., Blockley, S.P.E., Blunier, T., Buchardt, S.L., Clausen, H.B., Cvijanovic, I., Dahl-Jensen, D., Johnsen, S.J., Fischer, H., Gkinis, V., Guillevic, M., Hoek, W.Z., Lowe, J.J., Pedro, J., Popp, T., Seierstad, I., Steffensen, J.P., Svensson, A.M., Vallelonga, P., Vinther, B.M., Walker, M.J.C., Wheatley, J.J., Winstrup, M., 2014. A framework for robust naming and correlation of past abrupt climatic changes during the recent glacial period based on three synchronised Greenland ice-cores. Quat. Sci. Rev. 106, 14–28.
Rasmussen, T.L., Balbon, E., Thomsen, E., Labeyrie, L., van Weering, T.C.E., 1999. Climate records and changes in deep outflow from the Norwegian Sea similar to 150-55 ka. Terra Nova 11, 61–66.
Rasmussen, T.L., Wastegård, S., Kuijpers, A., van Weering, T.C.E., Heinemeier, J., Thomsen, E., 2003. Stratigraphy and distribution of tephra layers in marine sediment cores from the Faeroe Islands, North Atlantic. Mar. Geol. 199, 263–277.
Ruth, U., Barnola, J.M., Beer, J., Bigler, M., Blunier, T., Castellano, E., Fischer, H., Fundel, F., Huybrechts, P., Kaufmann, P., Kipfstuhl, S., Lambrecht, A., Morganti, A., Oerter, H., Parrenin, F., Rybak, O., Severi, M., Udisti, R., Wilhelms, F., Wolff, E., 2007. "EDML1": a chronology for the EPICA deep ice core from Dronning Maud Land, Antarctica, over the last 150 000 years. Clim. Past 3, 475–484.
Sanchez Goni, M.F., Bard, E., Landais, A., Rossignol, L., d/'Errico, F., 2013. Air-sea temperature decoupling in western Europe during the Last Interglacial-Glacial transition. Nat. Geosci. 6, 837–841.
Seierstad, I.K., Abbott, P.M., Bigler, M., Blunier, T., Bourne, A.J., Brook, E., Buchardt, S.L., Buizert, C., Clausen, H.B., Cook, E., Dahl-Jensen, D., Davies, S.M., Guillevic, M., Johnsen, S.J., Pedersen, D.S., Popp, T.J., Rasmussen, S.O., Severinghaus, J., Svensson, A., Vinter, B.M., 2014. Consistently dated records from the Greenland GRIP, GISP2 and NGRIP ice-cores for the past 104 ka reveal regional millennial-scale isotope gradients 2 with possible Heinrich Event imprint. submitted for publication Quat. Sci. Rev. 106, 29–46.
Sejrup, H.P., Sjøholm, J., Furnes, H., Beyer, I., Eide, L., Jansen, E., Mangerud, J., 1989. Quaternary tephrochronology on the Iceland Plateau, north of Iceland. J. Quat. Sci. 4, 109–114.
Severi, M., Becagli, S., Castellano, E., Morganti, A., Traversi, R., Udisti, R., Ruth, U., Fischer, H., Huybrechts, P., Wolff, E., Parrenin, F., Kaufmann, P., Lambert, F., Steffensen, J.P., 2007. Synchronisation of the EDML and EDC ice cores for the last 52 kyr by volcanic signature matching. Clim. Past 3, 367–374.
Shackleton, N.J., Chapman, M., Sanchez-Goni, M.F., Pailler, D., Lancelot, Y., 2002. The Classic Marine Isotope Substage 5e. Quat. Res. 58, 14–16.
Shackleton, N.J., Hall, M.A., Vincent, E., 2000. Phase relationships between millennial-scale events 64,000-24,000 years ago. Paleoceanography 15, 565–569.
Siddall, M., Rohling, E.J., Blunier, T., Spahni, R., 2010. Patterns of millennial variability over the last 500 ka. Clim. Past 6, 295–303.
Sjøholm, J., Sejrup, H.P., Furnes, H., 1991. Quaternary volcanic ash zones on the Iceland Plateau, southern Norwegian Sea. J. Quat. Sci. 6, 159–173.
Steffensen, J.-P., 1995. Microparticles and Chemical Impurities in ice Cores from Dye-3, South Greenland, and their Interpretation in Palaeoclimatic Reconstructions. Niels Bohr Institute. University of Copenhagen.

Sun, S.S., McDonough, W.F., 1989. Chemical and isotopic systematics of oceanic basalts: implications for mantle composition and process. In: Saunders, A.D., Norry, M.J. (Eds.), Magmatism in Ocean Basins, Geological Society of London, Special Publication, pp. 313–345.

Svensson, A., Andersen, K.K., Bigler, M., Clausen, H.B., Dahl-Jensen, D., Davies, S.M., Johnsen, S.J., Muscheler, R., Parrenin, F., Rasmussen, S.O., Röthlisberger, R., Seierstad, I., Steffensen, J.P., Vinther, B.M., 2008. A 60 000 year Greenland stratigraphic ice core chronology. Clim. Past 4, 47–57.

Svensson, A., Bigler, M., Blunier, T., Clausen, H.B., Dahl-Jensen, D., Fischer, H., Fujita, S., Goto-Azuma, K., Johnsen, S.J., Kawamura, K., Kipfstuhl, S., Kohno, M., Parrenin, F., Popp, T., Rasmussen, S.O., Schwander, J., Seierstad, I., Severi, M., Steffensen, J.P., Udisti, R., Uemura, R., Vallelonga, P., Vinther, B.M., Wegner, A., Wilhelms, F., Winstrup, M., 2013. Direct linking of Greenland and Antarctic ice cores at the Toba eruption (74 ka BP). Clim. Past 9, 749–766.

Todd, J.A., Austin, W.E.N., Abbott, P.M., 2014. Quantifying bioturbation in a simulated ash fall event. In: Austin, W.E.N., Abbott, P.M., Davies, S.M., Pearce, N.J.G., Wastegård, S. (Eds.), Marine Tephrochronology, Geological Society, London, Special Publications, 398.

Turney, C.S.M., 1998. Extraction of rhyolitic ash from minerogenic lake sediments. J. Paleolimnol. 19, 199–206.

Wallrabe-Adams, H.-J., Lackschewitz, K.S., 2003. Chemical composition, distribution, and origin of silicic volcanic ash layers in the Greenland-Iceland-Norwegian Sea: explosive volcanism from 10 to 300 ka as recorded in deep-sea sediments. Mar. Geol. 193, 273–293.

Wastegård, S., Björck, S., Grauert, M., Hannon, G.E., 2001. The Mjáuvøtn tephra and other Holocene tephra horizons from the Faroe Islands: a link between the Icelandic source region, the Nordic Seas and the European continent. Holocene 11, 101–109.

Wastegård, S., Björck, S., Greve, C., Rasmussen, T.L., 2005. A tephra-based correlation between the Faroe Islands and the Norwegian Sea raises questions about chronological relationships during the last interglacial. Terra Nova, 1–6.

Wastegård, S., Rasmussen, T.L., 2001. New tephra horizons from Oxygen Isotope Stage 5 in the North Atlantic: correlation potential for terrestrial, marine and ice-core archives. Quat. Sci. Rev. 20, 1587–1593.

Wolff, E.W., Chappellaz, J., Blunier, T., Rasmussen, S.O., Svensson, A., 2010. Millennial-scale variability during the last glacial: the ice core record. Quat. Sci. Rev. 29, 2828–2838.

Wolff, E.W., Cook, E., Barnes, P.R.F., Mulvaney, R., 2005. Signal variability in replicate ice cores. J. Glaciol. 51, 462–468.

Zielinski, G.A., Mayewski, P.A., Meeker, L.D., Grönvold, K., Germani, M.S., Whitlow, S., Twickler, M.S., Taylor, K., 1997. Volcanic aerosol records and tephrochronology of the Summit, Greenland, ice cores. J. Geophys. Res. 102, 26,625–26,640.

Zielinski, G.A., Mayewski, P.A., Meeker, L.D., Whitlow, S., Twickler, M.S., 1996. A 110,000 year record of explosive volcanism from the GISP2 (Greenland) ice core. Quat. Res. 45, 109–118.